Accepted Manuscript

Enteric Delivery of Regenerating Family Member 3 alpha Alters the Intestinal Microbiota and Controls Inflammation in Mice With Colitis

Marion Darnaud, Alexandre Dos Santos, Patrick Gonzalez, Sandrine Augui, Claire Lacoste, Christophe Desterke, Gert De Hertogh, Emma Valentino, Emilie Braun, Jinzi Zheng, Raphael Boisgard, Christel Neut, Laurent Dubuquoy, Franck Chiappini, Didier Samuel, Patricia Lepage, Francesca Guerrieri, Joel Doré, Christian Bréchot, Nicolas Moniaux, Jamila Faivre

PII: S0016-5085(17)36349-7
DOI: 10.1053/j.gastro.2017.11.003
Reference: YGAST 61532

To appear in: *Gastroenterology*
Accepted Date: 6 November 2017

Please cite this article as: Darnaud M, Santos AD, Gonzalez P, Augui S, Lacoste C, Desterke C, De Hertogh G, Valentino E, Braun E, Zheng J, Boisgard R, Neut C, Dubuquoy L, Chiappini F, Samuel D, Lepage P, Guerrieri F, Doré J, Bréchot C, Moniaux N, Faivre J, Enteric Delivery of Regenerating Family Member 3 alpha Alters the Intestinal Microbiota and Controls Inflammation in Mice With Colitis, *Gastroenterology* (2017), doi: 10.1053/j.gastro.2017.11.003.

Enteric Delivery of Regenerating Family Member 3 alpha Alters the Intestinal Microbiota and Controls Inflammation in Mice With Colitis

Marion Darnaud,[1,2,11] **Alexandre Dos Santos**,[1,2,11] **Patrick Gonzalez**,[1,2,11] Sandrine Augui,[1,2] Claire Lacoste,[1,2] Christophe Desterke,[2] Gert De Hertogh,[3] Emma Valentino,[1,2] Emilie Braun,[1,2] Jinzi Zheng,[4,5,#] Raphael Boisgard,[4,5] Christel Neut,[6] Laurent Dubuquoy,[6] Franck Chiappini,[1,2] Didier Samuel,[1,2] Patricia Lepage,[7] Francesca Guerrieri,[8] Joel Doré,[7] Christian Bréchot,[1,2,9] Nicolas Moniaux,[1,2] and Jamila Faivre[1,2,10,*]

[1]INSERM, U1193, Paul-Brousse University Hospital, Hepatobiliary Centre, Villejuif 94800, France

[2]Univ. Paris-Sud, Université Paris-Saclay, Faculté de Médecine Le Kremlin-Bicêtre, France

[3]Department of Imaging and Pathology, Unit of Translational Cell and Tissue Research, University of Leuven, 3000 Leuven, Belgium

[4]CEA, DSV, Institut d'Imagerie Biomédicale, Orsay 91400, France

[5]INSERM, U1023, Université Paris Sud, Orsay 91400, France

[6]LIRIC-U995, Univ. Lille, Inserm, CHU Lille, Lille, France.

[7]Institut National de la Recherche Agronomique, UMR 1319 MICALIS, Jouy-en-Josas 78352, France,

[8]Center for Life NanoScience@Sapienza, Istituto Italiano di Tecnologia, Roma 00197, Italy

[9] Pasteur Institute, Paris, France

[10]Assistance Publique-Hôpitaux de Paris (AP-HP), Pôle de Biologie Médicale, Paul-Brousse University Hospital, Villejuif, France

[11]Authors share co-first authorship.

[#]Present Address: Institute of Biomaterials & Biomedical Engineering, University of Toronto, Ontario M5G 1L7, Canada

Correspondence

Address requests for reprints to: Jamila Faivre, MD, PhD, INSERM U1193, University Paris-Sud-Paris Saclay, Paul-Brousse Hospital, Hepatobiliary Centre, 14 Av. Paul Vaillant-Couturier, Villejuif 94800, France. fax: +3314559026

Conflicts of interest: The authors disclose no conflicts.

Running title: REG3A alters gut microbiota and controls inflammation in mice with colitis

Abbreviations used in this paper: AMPs, antimicrobial peptides/proteins; CCL, C-C Motif Chemokine ligand; CFUs, colony forming units; DSS, dextran sodium sulphate; HIP/PAP, Hepatocarcinoma-Intestine-Pancreas/Pancreatitis Associated Protein; IBD, inflammatory bowel disease; IL, interleukin; FISH, fluorescence *in situ* hybridization; GIT, gastrointestinal tract; LPS, lipopolysaccharide endotoxin; MDA, malondialdehyde; PCA, Principal component analysis; REG3, Regenerating islet-derived protein 3; ROS, Reactive Oxygen Species; TNBS, 2,4,6-trinitrobenzene sulfonic acid; TNFα; Tumor Necrosis Factor α; WT, wild-type.

Author contribution

MD, ADS and PG share co-first authorship.

Study concept: M. Darnaud, C. Bréchot, J. Faivre.

Experiment design and data acquisition: M. Darnaud, A. Dos Santos, P. Gonzalez, S. Augui, C. Lacoste, E. Valentino, E. Braun, J. Zheng, R. Boisgard, C. Neut, L. Dubuquoy, F. Guerrieri, N. Moniaux, J. Faivre.

All the authors contributed to the analysis and interpretation of data.

Supervising the study, obtaining fundings and drafting the manuscript: J. Faivre.

Funding: This work was supported by grants from the Fondation ARC pour la Recherche sur le Cancer (PJA 20111203952, PJA 20131200221, PJA 20141202048 and PJA 20111203952). S.A. was funded by a Association pour la Recherche sur le Cancer Fellowship (R12036LL). J.F. was supported by the European Union's Seventh Framework Programme (FP7) under grant agreement No. 259743 (MODHEP consortium), the Institut National du Cancer, the OSEO-BPI Programme d'Investissements d'Avenir (IMODI and HECAM consortiums; R14035LB and R15065LH, respectively).

Acknowledgements We warmly thank Dr. H. Blottière, Professor F. Carbonnel, Professor J.F. Colombel and Dr. P. Langella for fruitful discussions. For experimental assistance, we thank R. Duchateau, Dr. C. Martin and Dr K. Lipson (animal care), F. Levenez (gnotobiology, 16S DNA extraction), L. Calvo (16S rDNA libraries), C. Bridonneau (anaerobic bacterial strains), Dr. P. Le Baccon (fluorescence microscopy), P. Duchambon (recombinant proteins), the Alfact Innovation Company (ALF5755 recombinant protein), the IGBMC Platform (microarray), the CLNS@Sapienza genomics Platform (sequencing) and the INRA GenoToul Bioinformatics Facility (computing and storage resources).

Summary

Background & Aims

Paneth cell dysfunction causes deficiencies in intestinal C-type lectins and antimicrobial peptides, which leads to dysbiosis of the intestinal microbiota, alters the mucosal barrier, and promotes development of inflammatory bowel diseases. We investigated whether transgenic expression of the human regenerating family member 3 alpha gene (*REG3A*) alters the fecal microbiota and affects development of colitis in mice.

Methods

We performed studies with C57BL/6 mice that express human regenerating family member 3 alpha (hREG3A) in hepatocytes, via the albumin gene promoter. In these mice, hREG3A travels via the bile to the intestinal lumen. Some mice were given dextran sodium sulphate (DSS) to induce colitis. Feces were collected from mice and the composition of the microbiota was analyzed by 16S rRNA sequencing. The fecal microbiome was also analyzed from mice that express only 1 copy of human *REG3A* transgene but were fed feces from control mice (not expressing hREG3A) as newborns. Mice expressing hREG3A were monitored for DSS-induced colitis after cohousing or feeding feces from control mice. Colitis was induced in another set of control and hREG3A transgenic mice by administration of trinitrobenzene sulfonic acid; some mice were given intrarectal injections of the hREG3A protein. Colon tissues were collected from mice and analyzed by histology and immunohistochemistry to detect mucin 2, as well as by 16S rRNA fluorescence in situ hybridization, transcriptional analyses, and quantitative PCR. We measured levels of reactive oxygen species (ROS) in bacterial cultures and fecal microbiota using H2-DCFDA and flow cytometry.

Results

The fecal microbiota of mice that express hREG3A had a significant shift in composition, compared to control mice, with enrichment of Clostridiales (Ruminococcaceae, Lachnospiraceae) and depletion of Bacteroidetes (Prevotellaceae); the transgenic mice developed less-severe colitis following administration of DSS than control mice, associated with preserved gut barrier integrity and reduced bacterial translocation, epithelial inflammation, and oxidative damage. A similar shift in the composition of the fecal microbiota occurred after a few months in transgenic mice heterozygous for *REG3A* that harbored a wild-type maternal microbiota at birth; these mice developed less-severe forms of colitis following DSS administration. Cohoused and germ-free mice fed feces from *REG3A* transgenic mice and given DSS developed less-severe forms of colitis and had reduced lipopolysaccharide activation of the toll-like receptor 4 and increased survival times compared to mice not fed feces from *REG3A* transgenic mice. *REG3A* transgenic mice developed only mild colonic inflammation after exposure to trinitrobenzene sulfonic acid (TNBS), compared to control mice. Control mice given intrarectal hREG3A and exposed to TNBS showed less colon damage and inflammation than mice not given intrarectal hREG3A. Fecal samples from *REG3A* transgenic mice had lower levels of ROS than feces from control mice during DSS administration. Addition of hREG3A to bacterial cultures reduced levels of ROS and increased survival of oxygen-sensitive commensal bacteria (*Faecalibacterium prausnitzii* and *Roseburia intestinalis*).

Conclusions

Mice with hepatocytes that express human REG3A, which travels to the intestinal lumen, are less sensitive to colitis than control mice. We found hREG3A to alter the colonic microbiota by decreasing levels of ROS. Fecal microbiota from *REG3A* transgenic mice protect non-transgenic mice from induction of colitis. These findings indicate a role for reduction of oxidative stress in preserving the gut microbiota and its ability to prevent inflammation.

Keywords: mouse model, IBD, bacteria, LPS

Introduction

An abnormal gut microbiota composition (dysbiosis) and defective antimicrobial mucosal barrier are important pathogenic factors for inflammatory bowel diseases (IBD)[1]. Dysbiosis was reported to occur prior to clinical symptoms in pediatric Crohn's disease, suggesting that dysbiosis contributed to disease onset in genetically susceptible individuals[2]. Dysbiosis associated with IBD generally consists of shifts in relative abundance of specific bacterial communities favoring potentially harmful aerobic and facultative anaerobic bacteria to the detriment of beneficial strict anaerobic ones[3]. There is accumulating evidence that these shifts result from the oxidative nature of the host inflammatory response[4,5]. The selection mechanism is that oxidized by-products of the host inflammatory response feed aerobic and facultative anaerobic bacteria, while the strict anaerobic bacteria, which lack Reactive Oxygen Species (ROS) detoxifying enzymes, are killed. Oxidative stress in the gastrointestinal tract (GIT) is thus closely linked to dysbiosis during IBD and non-IBD gut disorders and might be an important therapeutic target[6,7].

Another key contributor to dysbiosis and mucosal barrier impairment during IBD is a deficiency in the secretion of antimicrobial proteins (AMPs) such as defensins, cathelicidins and C-type lectins resulting notably from Paneth cell dysfunction[8]. This enteric arsenal forms part of innate immunity, contributing to a balanced clearance of pathogens and tolerance of commensal microbes in the gut[8,9]. In mice, an over-expression, or an oral administration, of an enteric defensin led to significant changes in gut microbiota composition; however, the underlying mechanisms and the health benefits provided by these changes remain to be demonstrated[10,11]. In fact, AMPs display multiple biological activities, each of which might influence the host-microbiota interplay[12], but those by which they actually regulate the gut

microbiota composition and function are little known. In particular, the way in which the antimicrobial properties of AMPs interact with such a complex ecosystem as the gut microbial communities remains unclear given that these antimicrobial properties are counteracted by various mechanisms of bacterial resistance that maintain homeostasis[13,14]. Moreover, an individual antimicrobial molecule only targets a narrow bacterial spectrum, so that a broad range of them must act simultaneously to ensure selection pressure on the gut microbiota[15]. The structure and function of some antimicrobial molecules are sensitive to environmental factors, such as pH and redox potential[16-18], entailing that a given set of molecules exerts different selection pressures in homeostatic or inflammatory states.

The human secreted C-type lectin hREG3A, or Hepatocarcinoma-Intestine-Pancreas/Pancreatitis Associated Protein (HIP/PAP), is a 16 kDa carbohydrate-binding protein exhibiting remarkable anti-inflammatory activities in many eukaryote cell types, where hREG3A promotes tissue regeneration and repair[19-25]. It is expressed in Paneth's cells and the neuroendocrine cells of the small intestine physiologically, and in the large intestine in response to infection and inflammation. The mechanisms of reduction of inflammation by hREG3A are not fully understood. hREG3A is a potent ROS scavenger and its tissue protective and regenerative effects are largely due to this antioxidant property[19,20,25]. hREG3A and its murine homologue Reg3g also display antibacterial activities against Gram-positive bacteria by interacting with peptidoglycan carbohydrate[26]. Reg3b, another murine homologue of hREG3A, exerts bactericidal activity against Gram-negative bacteria by binding to lipopolysaccharide[27-29]. Strain differences in susceptibility of Gram-positive bacteria to hREG3A have been reported[30,31], suggesting that the antibacterial spectrum of the REG3 proteins might be relatively narrow.

In this study, we investigated the effects of an enteric delivery of the human REG3A protein on gut microbiota homeostasis and the response to inflammation in mice. We showed that

hREG3A changed the gut microbiota composition (enrichment of Clostridiales, depletion of Bacteroidetes and Proteobacteria), decreased the oxidative stress and inflammatory response of the gut epithelium and reduced host susceptibility to colitis. hREG3A lowered ROS levels in the gut microbiota of mice with colitis and increased the viability of some Gram-positive oxygen-sensitive Clostridia *in vitro* indicating that the antioxidant activity of hREG3A contributed to shaping the gut microbiota. This study offers a new paradigm for regulation of the host-microbiota interplay based on the ROS scavenging activity of an innate immune molecule.

Materials and Methods

Animal studies

Animal studies were performed in compliance with the institutional and European Union guidelines for laboratory animal care and approved by the Ethics Committee of CE2A-03-CNRS-Orléans (Accreditation N°01417.01). Homozygous transgenic C57BL/6 mice expressing *REG3A* in hepatocytes under the control of the mouse albumin gene promoter were derived from a strain previously produced in our laboratory[32]. The cohousing experiments were performed with 3-week-old weaned WT mice randomly cohoused with age-matched *REG3A*-transgenic mice at a 1:1 ratio for 8 weeks. Ten-week-old germ-free mice underwent two gastric gavages at 48h intervals using inocula consisting of pooled fresh feces from 8 *REG3A*-transgenic or WT mice.

DSS colitis

Colitis was induced in mice with a 3% 40kDa dextran sodium sulphate (DSS) solution (TdB Consultancy AB), which was added to their drinking water for 5 days followed by ad libitum access to tap water for 7 days.

TNBS colitis

Overnight-fasted mice were anesthetized for 90 min and received intrarectally 150 mg/kg of 2,4,6-trinitrobenzene sulfonic acid (TNBS; Sigma-Aldrich) together with ethanol. WT mice received an intrarectal injection of 100µg of a recombinant hREG3A protein on the day before and on the day of TNBS administration.

16S rRNA analysis

DNA pyrosequencing of the V3-V4 hypervariable region of 16S rRNA gene was performed using the Illumina Miseq instrument. The sequences thus generated were pre-processed using the mothur pipeline and then clustered into OTUs based on 97% of similarity. RDP release 11 was used as reference database. Principal Component Analyses (PCA) were performed based on bacterial family and genera compositions using the R packages ade4 and FactoMiner.

Bacterial strains, culture conditions and ROS quantification

The bacterial strains used were *Enterococcus faecalis* (ATCC-19433), *Faecalibacterium prausnitzii* A2-165 (DSM17677) and *Roseburia intestinalis* L1-82 (DSM14610T). Oxidative stress was induced by addition of 200mM Paraquat (1,1′-dimethyl-4,4′-bipyridinium dichloride; Sigma Aldrich), which is commonly used experimentally to generate superoxide radical, hydrogen peroxide and hydroxyl radical in cells[33]. Intracellular ROS levels and cell viability were determined by flow cytometry with 2′,7′-dichlorofluorescein diacetate (H_2-DCFDA) and propidium iodide in bacteria cultures. Bacterial growth was assessed by Colony Forming Unit (CFU) counting on agar plates. Bacterial ROS levels in fresh fecal microbiota were measured by flow cytometry with H_2-DCFDA.

Other Methods

For histology, immunohistochemistry, recombinant protein production, Elisa assays, immunoblotting, dot-blot, fluorescence in-situ hybridization, transcriptomics, and [^{18}F]FDG PET scan, please see details in the Supplementary Materials and Methods.

Statistics

Results are presented as means ± SEM or box plots. Differences between sample groups were tested using non-parametric Wilcoxon rank sum (two-sided) for all the experiments reported, except for: two-way ANOVA tests were used for the in-vivo quantifications of [^{18}F]FDG and H_2-DCFDA over time; the robustness of Principal Component Analysis clustering was assessed with a Monte-Carlo rank test; the Kaplan-Meier survival analysis with a log-rank test was applied to compare the time course of survival between the groups. *P*-values <0.05 were deemed statistically significant.

Results

Human REG3A delivered into the gut lumen shifts the gut microbiota composition in hepatocyte-targeted *REG3A* transgenic mice

We studied the effects of human REG3A on gut microbiota composition and gut barrier integrity in mice transgenic for *REG3A* under homeostatic and inflammatory conditions. Inflammation was induced by oral absorption of dextran sodium sulphate (DSS). To prevent degradation of the hREG3A protein by acid and luminal proteases in the upper GIT, we used previously generated homozygous transgenic C57BL/6 mice expressing *REG3A* in hepatocytes under the control of the mouse albumin gene promoter[32] and showed that, in these mice, hREG3A flowed into bile ducts and the GIT lumen (Figure 1*A, B* and *D*). Transgenic hepatocytes secreted hREG3A into blood vessels through the basolateral membranes, and into bile canaliculi through the apical membranes. The expression levels of endogenous Reg3b and Reg3g in the blood and colon tissues were negligible in the basal state of wild-type (WT) mice and high after DSS administration (Figure 1*A* and *C*). In *REG3A*-transgenic mice, a similar high serum level of hREG3A was found in the basal and inflammatory states (Figure 1*A*). This level was similar to that of the endogenous Reg3 in WT mice with colitis. The colon expression levels of the endogenous Reg3 mRNAs were

negligible in both the basal and inflammatory states of *REG3A*-transgenic mice (Figure 1*C*). In other words, *REG3A*-transgenic mice did not display any up-regulation of Reg3b or Reg3g during colitis (perhaps because they were retro-controlled by the over-expressed *REG3A*), implying that Reg3b and Reg3g played a negligible part in *REG3A*-transgenic mice. We analysed the fecal microbiota composition in healthy and DSS-given *REG3A*-transgenic mice using MiSeq 16S rDNA gene sequencing. Control WT and *REG3A*-transgenic mice were bred and processed under the same conditions. Principal component analysis (PCA) revealed two clearly separate clusters for *REG3A*-transgenic and WT mice at the family level both before (P=0.001) and after (P=0.039) exposure to DSS (Figure 1*E* and Supplementary Figure 1*A*). Twelve bacterial families displayed significant differences in their relative abundance between *REG3A*-transgenic and WT mice in either the basal or inflammatory state, or both (Figure 1*F*). *Sutterellaceae* (phylum Proteobacteria), *Prevotellaceae*, *Porphyromonadaceae* and *Bacteroidaceae* (phylum Bacteroidetes) were under-represented, while *Lachnospiraceae* and unclassified *Clostridia* (phylum Firmicutes) were over-represented in the basal state of *REG3A*-transgenic mice compared to that of WT mice (Figure 1*F*). The same shifts in microbial composition were found at the genus level (Supplementary Figure 1*B*). In the inflammatory, compared to basal, state, WT mice displayed an enrichment of *Prevotellaceae* and unclassified *Bacteroidales* and a depletion of *Porphyromonadaceae*, *Sutterellaceae* and unclassified *Desulfovibrionales*, while *REG3A*-transgenic mice displayed an increase in *Prevotellaceae*, unclassified *Bacteroidales*, *Bacteroidaceae* and *Verrucomicrobiaceae* and a decrease in *Lactobacillaceae*, unclassified *Clostridia* and *Lachnospiraceae*. DSS-given *REG3A*-transgenic mice exhibited a lower level of *Prevotellaceae* and a much higher level of *Ruminococcaceae* (order Clostridiales) (Figure 1*F* and Supplementary Figure 1*C*) than DSS-given WT mice. We then investigated whether the gut microbiota composition of homozygous transgenic (REG3A-TG+/+) mice at baseline was due to the *REG3A* transgene

or an extra-genetic effect[34]. We studied the time evolution of the microbiota in mice that expressed only 1 copy of human *REG3A* transgene (REG3A-TG+/-), were born to WT mothers and initially had the maternal microbiota. The fecal microbiomes of 15 REG3A-TG+/- pups from three different litters and cages were sequenced at the ages of 9 and 12 weeks and compared to those of their WT dams (n=3) and unrelated WT mice of similar ages (n=11). The fecal microbiomes of twelve REG3A-TG+/+ mice were analysed for comparison. PCA plots at the family level showed that the microbiota from REG3A-TG+/- mice were grouped in between those from (maternal and unrelated) WT and REG3A-TG+/+ mice at 9 weeks (P<0.01 for REG3A-TG+/- *vs* WT and REG3A-TG+/- *vs* REG3A-TG+/+) and moved close to those from REG3A-TG+/+ mice during the next three weeks (P<0.001 for REG3A-TG+/- *vs* WT; P>0.05 for REG3A-TG+/- *vs* REG3A-TG+/+) (Figure 1*G*). The microbiota composition shift of the REG3A-TG+/- mice compared to the microbiota of WT mice mostly consisted of a decrease in *Prevotellaceae*, *Sutterellaceae* and *Verrucomicrobiaceae* and an increase in *Lachnospiraceae* and *Ruminococcaceae*, to reach levels comparable to those of REG3A-TG+/+ mice after 12 weeks (Figure 1*H*). Thus the WT microbiota of the *REG3A* heterozygous newborns evolved toward a transgenic-positive microbiota in a few months, which means that the *REG3A* transgene effect superseded the maternal legacy.

hREG3A increases the viability of some highly oxygen-sensitive Clostridia

The shift in microbiota composition in *REG3A*-transgenic mice compared to WT mice corresponded to a large increase in the ratio between Gram-positive and Gram-negative bacteria (Figure 2*A*), difficult to reconcile with the reported selective anti-Gram-positive bactericidal activity of hREG3A[26]. We conjectured that the antioxidant activity of hREG3A was a key factor in shifting the intestinal microbial ecology in *REG3A*-transgenic mice. The mechanism at play would be a selection pressure exerted by hREG3A in favor of strict

anaerobic Gram-positive bacteria, as are some Clostridia. To substantiate this view, we measured ROS levels in fresh fecal microbiota of WT and *REG3A*-transgenic mice using H_2-DCFDA and flow cytometry over the five-day period of DSS administration, during which the gut barrier was not yet damaged nor colitis established. The ROS levels at d1 of DSS administration were similar to the baseline level and then increased over time in both mouse lines. However, the rate of increase was significantly lower for the microbiota of *REG3A*-transgenic mice (P=0.02 over the d1-d5 time period), evidencing a ROS scavenging activity of the *REG3A* transgene in a microbiota subjected to an oxidative stress (Figure 2*B*). We also tested the antioxidant efficiency of a full-length recombinant human REG3A protein (rcREG3A) in prokaryote cells *in vitro*. The recombinant protein we used is chemically and biologically active in terms of anti-inflammatory properties in eukaryotic cells and carbohydrate binding selectivity[10,20,25] (Supplementary Figure 2). We cultured Gram-positive *Enterococcus faecalis* stressed with a ROS generator (paraquat) during the exponential phase of growth. Exposure to 200mM paraquat had a strong bactericidal effect on *E. faecalis*. The addition of 10µM rcREG3A restored the exponential growth of *E. faecalis*, suggesting that the ROS generated by paraquat were effectively reduced by rcREG3A (Figure 2*C*). This was demonstrated by flow cytometry using the ROS-specific fluorescent probe H_2-DCFDA and propidium iodide DNA staining (Figure 2*D* and *E* and Supplementary Figure 3). We found some bacterial aggregation, but no bactericidal effect of rcREG3A on *E. faecalis* (Figure 2*C*), at variance with previous reports[26]. This discrepancy may rely on many factors pertaining to the protein[26] or the bacterial strain[30,31], but note that an absence of bactericidal activity of hREG3A would be consistent with the enrichment of Gram-positive bacteria we observed in the gut microbiota of *REG3A*-transgenic mice compared to that of WT mice. We cultured of two well-documented extremely oxygen sensitive Gram-positive bacteria species, *Roseburia intestinalis* (*Lachnospiraceae*, Clostridium Cluster XIVa) and *Faecalibacterium prausnitzii*

(*Ruminococcaceae*, Clostridium Cluster IV), which are major butyrate producers dramatically reduced during IBD[35-38]. *R. intestinalis* is known to survive for less than 2 min when exposed to air on the surface of agar plates[39]. *F. prausnitzii* is more sensitive to air exposure than *R. intestinalis* and grows slowly even under anaerobic conditions[40]. We performed anaerobic cultures of *R. intestinalis* and *F. prausnitzii* followed, or not, by a 5-min exposure to ambient air. We found that rcREG3A had a significant growth-promoting effect on *F. prausnitzii* under strict anaerobic conditions and a survival effect on both bacteria after exposure to oxygen (Figure 2*F* and *G*). The centrifugation of *F. prausnitzii* anaerobic cultures incubated with rcREG3A for 24h, followed by anti-hREG3A immunoblotting, showed that a 15-kDa rcREG3A co-sedimented with bacterial aggregates (Supplementary Figure 4*A*). Slide-mounted imaging showed that *F. prausnitzii* incubated with rcREG3A survived, whereas control cultures were completely lysed, after 2h of exposure to ambient air (Supplementary Figure 4*B*). These findings establish that rcREG3A exerts a potent antioxidant activity on prokaryotic cells and is capable of increasing the viability and growth of some extremely oxygen-sensitive commensal Clostridia.

REG3A-transgenic mice are less susceptible to DSS- and TNBS-induced colitis than WT mice

The dysbiotic microbiota of patients with IBD is mostly characterized by an increase in *Sutterellaceae, Prevotellaceae,* and *Enterobacteriaceae* (phylum *Proteobacteria*) and a decrease in *Ruminococcaceae* and *Lachnospiraceae* (which include the principal butyrate-producing symbionts)[3,35-38], Similar shifts in the composition of the gut microbiota are also associated with colitis in genetically susceptible mouse models[41,42]. The fact that more or less reverse shifts occur in the gut microbiota of healthy *REG3A*-transgenic mice compared to WT mice suggests that a microbiota shaped by hREG3A might have a beneficial impact on health.

We therefore studied the response to induced colitis in *REG3A*-transgenic mice, and also performed feces transfer experiments. *REG3A*-transgenic mice received oral administrations of 3% DSS for 5 days followed by normal water for 7 days. Control groups of WT mice were bred and processed under the same conditions. Body weight changes, stool consistency and bleeding scores and survival rate were monitored over time. Histopathological features were scored on day 12. Strikingly, DSS-given *REG3A*-transgenic mice displayed only a very few signs of colitis. They had reduced weight loss, diarrhea and rectal bleeding compared to WT mice and had a 100% survival rate on day 12 compared to 70% in WT mice (Figure 3*A*-*D*). Their colons displayed fewer barrier defects and less Goblet cell loss and inflammatory cell infiltration than those of WT mice (Figure 3*E* and *F* and Supplementary Figure 5). Twelve-week-old REG3A-TG+/- mice born to WT mothers were also exposed to DSS. They exhibited a relatively benign colitis (Supplementary Figure 6*A*-*D*), consistent with the fact that their gut microbiota was similar in composition (Figure 1*G*), and thus functionality, to those of *REG3A* homozygous transgenic mice. We ensured that the hREG3A lectin did not interact with dextran *in vitro* (Supplementary Figure 2)[43], and that, therefore, the observed phenotype could not be attributed to a direct blocking of DSS toxicity by hREG3A. Positron emission tomography (PET) imaging with 2-[18F]fluoro-2-deoxy-D-glucose ([18F]FDG), a tracer for abnormally high glucose metabolism in inflammatory areas, was used to quantify intestinal inflammation. Colonic [18F]FDG uptake increased over time in WT mice with colitis whereas it remained weak (i.e. comparable to that seen in healthy) in *REG3A*-transgenic mice (P=0.013 over the d7-d12 time period) (Figure 3*G* and *H*). The severity of colitis was also assessed by measuring the colonic expression levels of inflammatory markers (*Il1a*, *Il1b*, *Tnf*, *Il6*, *Cxcl1*, *Ccl3*, *Ccl9*). Most of them showed a significant increase upon DSS administration in WT mice, and not in *REG3A*-transgenic mice (Figure 3*I*). We studied the integrity of the gut mucosal barrier in healthy and DSS-given *REG3A*–transgenic mice using

immunostaining for Muc2 mucin and 16S rRNA FISH, transcriptome profiling and gene set enrichment analysis (GSEA) with the KEGG and Reactome databases. In the basal state, mucosal barriers of *REG3A*-transgenic and WT mice were microscopically similar. However, several pathways related to the intestinal barrier, including modulators of cell-matrix interactions and mucin *O*-glycosylation, were upregulated in *REG3A*-transgenic mice (Supplementary Figure 7*A*). During intestinal inflammation, the colon mucosal barrier remained intact over considerable areas in *REG3A*-transgenic mice, whereas it was largely disrupted in WT mice, leading to bacterial colonization across the epithelium (Figure 4*A*). The functional robustness of the mucosal barrier in *REG3A*-transgenic, compared to WT, mice was further highlighted as follows. An up-regulation of some tight-junction genes involved in the regulation of cell-cell interactions was observed (Supplementary Figure 7*B*). An increase in *O*-glycosylation of epithelial mucins was revealed by wheat germ agglutinin (WGA) immunoblotting (Figure 4*B*). The level of bacterial translocation in mesenteric lymph nodes remained low, as shown by 16S rRNA FISH analysis (Figure 4*C*). A number of genes related to the lipopolysaccharide endotoxin (LPS)-induced activation pathway were downregulated in colon epithelial cells (Figure 4D). Unsupervised transcriptome analysis revealed a clustering of DSS-given *REG3A*-transgenic mice with healthy mice separately from DSS-given WT mice (Supplementary Figure S8). Consistent with this, the increase in inflammation-associated serum markers (LPS, soluble CD14) remained very small in these mice during intestinal inflammation (Figure 4*E* and *F*). Finally, the concentration of malondialdehyde (MDA), a biomarker of oxidative stress, in the colon tissue was substantially reduced in *REG3A*-transgenic, compared to WT, mice with colitis (Figure 4*G*). We then studied the susceptibility of *REG3A*-transgenic mice to an alternative type of colitis using a single intrarectal administration of trinitrobenzesulfonic acid (TNBS) together with ethanol. In contrast with oral administration of DSS, which destroys colon epithelial cells,

alters barrier function and subsequently causes inflammation, TNBS rapidly triggers a severe colonic inflammation through a T-cell immune response against haptenized proteins and luminal antigens[44]. We found that, two days after TNBS administration, *REG3A*-transgenic mice developed only mild colonic inflammation and mucosal damage (Figure 4*H*) associated with decreased levels of inflammatory cytokines (*Il1b*, *Tnf*) and myeloperoxidase (MPO) (Figure 4*I* and *J*).

The anti-inflammatory properties of gut microbiota shaped by hREG3A promote survival to DSS-induced colitis in colonized wild-type mice

To assess the protective action of hREG3A-shaped microbiota against colitis, we transferred fecal microbiota from *REG3A*-transgenic mice to WT mice by means of cohousing. Three-week-old weaned WT mice were cohoused with age-matched REG3A-transgenic mice for 8 weeks and then exposed to DSS. Control groups consisted of WT mice housed alone. At the end of the cohousing period, cohoused WT (CoH-WT) mice displayed a significant shift in gut microbiota composition towards a REG3A-transgenic profile at the bacteria family level (Figure 5*A*) and a clear alleviation of DSS-induced colitis compared to single-housed WT mice (Figure 5*B*-*G*). Next, we colonized germ-free C57BL/6 mice with a fecal microbiota from *REG3A*-transgenic (TG) or WT mice for 3 weeks. Formerly (Ex) germ-free (GF), but now colonized, mice will be designated as ExGF-TG or ExGF-WT according to the origin of the colonizing microbiota. The fecal microbiota was then analysed by sequencing (Day 0) and colonized mice were exposed to DSS. The microbiota of ExGF-TG and ExGF-WT mice at D0 had somewhat drifted from their respective inocula (Figure 5*H*). Nevertheless, the microbiota of ExGF-TG mice still harboured the same predominent bacterial communities as the inoculum, albeit with different relative abundance values, and remained far from that of ExGF-WT mice (Figure 5*H* and *I* and Supplementary Figure 7*A*-*E*). Upon DSS

administration, ExGF-TG mice exhibited a complete colitis survival in spite of transient signs of colitis, whereas 37% of the ExGF-WT mice died (Figure 5*J-M* and Supplementary Figure 8). This was associated with a reduced inflammatory response in terms of TLR4 signaling activation, colonic inflammatory markers and LPS-induced endotoxemia (Figure 5*N-P*). These results demonstrate a transmissible pro-survival action of the microbiota shaped by hREG3A probably due to a reduced inflammatory response in the gut epithelium and less systemic dissemination of gram-negative LPS. This is consistent with the depletion of potentially aggressive Gram-negative bacteria we observed in the gut microbiota shaped by hREG3A (Figure 2*A*).

Rectal use of a recombinant REG3A protein diminishes colonic inflammation in mice with TNBS-induced colitis

The fact that signs of colitis were partly reduced in CoH-WT and ExGF-TG mice while they were fully suppressed in *REG3A*-transgenic mice suggests that, in the latter, a direct interaction between over-expressed hREG3A and the host contributed to the maintenance of gut barrier homeostasis, in addition to the anti-inflammatory effects of the gut microbiota shaped by hREG3A. To substantiate this view, we evaluated the effects of intrarectal administrations of rcREG3A in WT mice with colitis. 100µg of rcREG3A (or an equivalent volume of buffer) was delivered on the day before and on the day of TNBS administration. The body weight loss was the same in the two groups of mice (Figure 6*A*). Histological stainings revealed that mice given intrarectal rcREG3A showed milder colonic barrier defects and inflammation than mice not given intrarectal rcREG3A (Figure 6*B* and Supplementary Figure S11). A significant decrease of the inflammatory markers *Il1b, Tnf* and MPO was observed in the colon tissues of mice given intrarectal rcREG3A (Figure 6*C*). These positive effects of a local administration of a recombinant REG3A protein makes it very likely that the

lower susceptibility to colitis observed in *REG3A*-transgenic mice was mostly due to the hepatic transgene REG3A traveling to the gut lumen, and not to a liver-dependent effect. They indicate that an exogenous hREG3A can contribute to the preservation of gut barrier integrity during colitis and underlines the potential human-health relevance of this molecule.

Discussion

Enteric innate immune molecules play an important role in gut barrier function and gut microbiota homeostasis through their pleiotropic activities. A reduced production of antimicrobial proteins resulting from a deregulation of the function of Paneth's cell may lead to dysbiosis and ultimately IBD[3]. A therapeutic approach consisting of increasing the intraluminal concentration of antimicrobial proteins in order to preserve host-microbiota homeostasis and thus prevent intestinal inflammation was proposed[45]. However preclinical models based on the enteric delivery of such biological agents were lacking because amongst other things of their proteolytic destruction in the upper digestive tract. The *REG3A*-transgenic mouse model we used enabled us to deliver a full-length human REG3A protein in the lower digestive tract lumen at sufficient doses to provide clear phenotypic effects in these mice, demonstrating the potential of an approach consisting of administering a large dose of exogenous REG3 to an organism already provided with an endogenous REG3-mediated response to intestinal inflammation[46]. The phenotypic features of *REG3A*-transgenic mice include significant changes in gut microbiota composition and a dramatic improvement of host resistance to intestinal inflammation, compared to control mice. *REG3A*-transgenic mice exposed to DSS exhibited very few signs of colitis, retained a tight mucosal barrier and achieved complete survival. The inflammatory response and the oxidative stress in the colon epithelium was much reduced in *REG3A*-transgenic, compared to WT, mice with DSS-induced colitis. A low level of inflammation and mucosal damage was also found in *REG3A*-transgenic mice with TNBS-induced colitis. The decrease in ROS levels in the fecal microbiota of *REG3A*-transgenic compared to control mice upon DSS exposure and the increase of survival to ambient-air exposure of highly oxygen sensitive bacteria cultured in the presence of rcREG3A demonstrate an antioxidant activity of hREG3A on prokaryotic cells that might modify host-microbiota interplay.

The microbial changes exhibited by *REG3A*-transgenic mice in homeostatic and inflammatory conditions mainly concerned an enrichment of Clostridiales (*Ruminococcaceae*, *Lachnospiraceae*) and a depletion of Bacteroidetes (*Prevotellaceae*). Mice heterozygous for *REG3A* that harbored a wild-type maternal microbiota at birth progressively acquired a gut microbiota composition close to that of *REG3A* homozygous transgenic mice – demonstrating the capability of hREG3A to shape the gut microbiota – and then exhibited a resistance to colitis similar to that of homozygous mice. The transfer of a hREG3A-shaped microbiota to wild-type mice by cohousing or faeces gavage resulted in a less severe disease, a reduced LPS-induced endotoxinemia and a higher survival to DSS exposure than in control groups, establishing the beneficial nature of the hREG3A-shifted microbiota composition. The phenotypic resistance was not fully transmitted by transfer experiments suggesting that hREG3A acted also by other ways, including direct mucosal effect, in *REG3A*-transgenic mice. Repeated intravenous administration of rcREG3A were ineffective, invalidating the hypothesis of a systemic anticolitogenic effect, whereas rectal administrations of rcREG3A helped to preserve gut barrier integrity during induced colitis in control mice.

Thus, hREG3A provides protection against inflammation and oxidative stress for both the intestinal epithelium and the commensal communities that form the gut microbiota. Future studies will be necessary to determine the sites involved in the ROS scavenging activity of hREG3A. Whether murine Reg3b and Reg3g encode proteins that carry similar antioxidant properties also needs to be determined.

Regarding the role of hREG3A in the host-gut microbiota interaction, we suggest that the broad-spectrum antioxidant activity of hREG3A may change the balance between different bacterial communities with different oxygen tolerances. In our mouse model, some highly oxygen-sensitive commensal bacteria could be responsive to an exogenous antioxidant such

as hREG3A, giving them a selective advantage over aerotolerant anaerobic ones, i.e. those developing an effective adaptive response to oxygen toxicity. In this hypothesis, hREG3A would shape the gut microbiota in the steady state through its antioxidant activity against the environmental stressors existing in the healthy gut and continue to exert this effect under inflammation and oxidative stress. This view is supported by the fact that hREG3A enhanced the growth of some highly oxygen-sensitive Clostridiales commensals. An enrichment of such symbionts may trigger a virtuous process by improving gut barrier function and reducing ROS production, which feeds back into benefiting symbionts. Conversely, an increase in Gram-negative commensal bacteria may trigger macrophage activation, increase ROS production, and amplify mucosal injuries and dysbiosis in favour of aerotolerant commensals. Our results suggest that the pressure exerted by hREG3A on the gut microbiota triggers such a virtuous shift in composition and functionality.

From a clinical viewpoint, our findings suggest that an increase in intraluminal concentration of hREG3A, for instance via a colon-targeted delivery method, may be a valuable approach to attenuate intestinal inflammation. Regarding the potential benefits to patients, such an approach would be a more physiological and nontoxic strategy for the treatment of inflammatory outbreaks than the available therapies. Moreover, it might be most successful in the early stages of the inflammatory process and could therefore be useful for the maintenance of medically- or surgically-induced remission and even the prevention of IBD in high-risk individuals.

References

1. Klag T, Stange EF, Wehkamp J. Defective antibacterial barrier in inflammatory bowel disease. Dig Dis 2013;31:310–316.
2. Gevers D, Kugathasan S, Denson LA, et al. The treatment-naive microbiome in new-onset Crohn's disease. Cell Host Microbe 2014;15:382–392.
3. Sartor RB, Wu GD. Roles for Intestinal Bacteria, Viruses, and Fungi in Pathogenesis of Inflammatory Bowel Diseases and Therapeutic Approaches. Gastroenterology 2017;152:327–339.e4.
4. Winter SE, Lopez CA, Bäumler AJ. The dynamics of gut-associated microbial communities during inflammation. EMBO Rep 2013;14:319–327.
5. **Albenberg L, Esipova TV**, Judge CP, et al. Correlation between intraluminal oxygen gradient and radial partitioning of intestinal microbiota. Gastroenterology 2014;147:1055–63.e8.
6. **Ballal SA, Veiga P, Fenn K**, et al. Host lysozyme-mediated lysis of Lactococcus lactis facilitates delivery of colitis-attenuating superoxide dismutase to inflamed colons. Proc Natl Acad Sci U S A 2015;112:7803–7808.
7. Dubourg G, Lagier J-C, Hüe S, et al. Gut microbiota associated with HIV infection is significantly enriched in bacteria tolerant to oxygen. BMJ open gastroenterology 2016;3:e000080.
8. Salzman NH, Bevins CL. Dysbiosis--a consequence of Paneth cell dysfunction. Semin Immunol 2013;25:334–341.
8. Zasloff M. Antimicrobial peptides of multicellular organisms. Nature 2002;415:389–395.
9. Vaishnava S, Yamamoto M, Severson KM, et al. The antibacterial lectin RegIIIgamma promotes the spatial segregation of microbiota and host in the intestine. Science

2011;334:255–258.

10. Salzman NH, Hung K, Haribhai D, et al. Enteric defensins are essential regulators of intestinal microbial ecology. Nat Immunol 2010;11:76–83.
11. Dupont A, Kaconis Y, Yang I, et al. Intestinal mucus affinity and biological activity of an orally administered antibacterial and anti-inflammatory peptide. Gut 2015;64:222–232.
12. Wang G. Human antimicrobial peptides and proteins. Pharmaceuticals (Basel) 2014;7:545–594.
13. Cullen TW, Schofield WB, Barry NA, et al. Gut microbiota. Antimicrobial peptide resistance mediates resilience of prominent gut commensals during inflammation. Science 2015;347:170–175.
14. Pang X, Xiao X, Liu Y, et al. Mosquito C-type lectins maintain gut microbiome homeostasis. Nature microbiology 2016;1:16023.
15. Juneja P, Lazzaro BP. Population genetics of insect immune responses. In: *Insect infection and immunity*. Oxford University Press; 2009:206–224.
16. Goldman MJ, Anderson GM, Stolzenberg ED, et al. Human beta-defensin-1 is a salt-sensitive antibiotic in lung that is inactivated in cystic fibrosis. Cell 1997;88:553–560.
17. Schroeder BO, Wu Z, Nuding S, et al. Reduction of disulphide bonds unmasks potent antimicrobial activity of human β-defensin 1. Nature 2011;469:419–423.
18. Abou Alaiwa MH, Reznikov LR, Gansemer ND, et al. pH modulates the activity and synergism of the airway surface liquid antimicrobials β-defensin-3 and LL-37. Proc Natl Acad Sci U S A 2014;111:18703–18708.
19. Moniaux N, Song H, Darnaud M, et al. Human hepatocarcinoma-intestine-pancreas/pancreatitis-associated protein cures fas-induced acute liver failure in mice by attenuating free-radical damage in injured livers. Hepatology 2011;53:618–627.

20. Moniaux N, Darnaud M, Garbin K, et al. The Reg3α (HIP/PAP) Lectin Suppresses Extracellular Oxidative Stress in a Murine Model of Acute Liver Failure. PLoS ONE 2015;10:e0125584.

21. Lieu H-T, Batteux F, Simon M-T, et al. HIP/PAP accelerates liver regeneration and protects against acetaminophen injury in mice. Hepatology 2005;42:618–626.

22. Lieu H-T, Simon M-T, Nguyen-Khoa T, et al. Reg2 inactivation increases sensitivity to Fas hepatotoxicity and delays liver regeneration post-hepatectomy in mice. Hepatology 2006;44:1452–1464.

23. Lai Y, Li D, Li C, et al. The antimicrobial protein REG3A regulates keratinocyte proliferation and differentiation after skin injury. Immunity 2012;37:74–84.

24. Lv Y, Yang X, Huo Y, et al. Adenovirus-mediated hepatocarcinoma-intestine-pancreas/pancreatitis-associated protein suppresses dextran sulfate sodium-induced acute ulcerative colitis in rats. Inflamm Bowel Dis 2012;18:1950–1960.

25. **Haldipur P, Dupuis N**, Degos V, et al. HIP/PAP prevents excitotoxic neuronal death and promotes plasticity. Ann Clin Transl Neurol 2014;1:739–754.

26. **Cash HL, Whitham CV**, Behrendt CL, et al. Symbiotic bacteria direct expression of an intestinal bactericidal lectin. Science 2006;313:1126–1130.

27. **Stelter C, Käppeli R**, König C, et al. Salmonella-induced mucosal lectin RegIIIβ kills competing gut microbiota. PLoS ONE 2011;6:e20749.

28. **Ampting MTJ van, Loonen LMP**, Schonewille AJ, et al. Intestinally secreted C-type lectin Reg3b attenuates salmonellosis but not listeriosis in mice. Infect Immun 2012;80:1115–1120.

29. Miki T, Holst O, Hardt W-D. The bactericidal activity of the C-type lectin RegIIIβ against Gram-negative bacteria involves binding to lipid A. J Biol Chem 2012;287:34844–34855.

30. Medveczky P, Szmola R, Sahin-Tóth M. Proteolytic activation of human pancreatitis-associated protein is required for peptidoglycan binding and bacterial aggregation. Biochem J 2009;420:335–343.

31. Loonen LMP, Stolte EH, Jaklofsky MTJ, et al. REG3γ-deficient mice have altered mucus distribution and increased mucosal inflammatory responses to the microbiota and enteric pathogens in the ileum. Mucosal Immunol 2014;7:939–947.

32. Simon M-T, Pauloin A, Normand G, et al. HIP/PAP stimulates liver regeneration after partial hepatectomy and combines mitogenic and anti-apoptotic functions through the PKA signaling pathway. FASEB J 2003;17:1441–1450.

33. Bus JS, Gibson JE. Paraquat: model for oxidant-initiated toxicity. Environ Health Perspect 1984;55:37–46.

34. Ubeda C, Lipuma L, Gobourne A, et al. Familial transmission rather than defective innate immunity shapes the distinct intestinal microbiota of TLR-deficient mice. J Exp Med 2012;209:1445–1456.

35. Souza HSP de, Fiocchi C. Immunopathogenesis of IBD: current state of the art. Nat Rev Gastroenterol Hepatol 2016;13:13–27.

36. Willing BP, Dicksved J, Halfvarson J, et al. A pyrosequencing study in twins shows that gastrointestinal microbial profiles vary with inflammatory bowel disease phenotypes. Gastroenterology 2010;139:1844–1854.e1.

37. **Quévrain E, Maubert MA, Michon C**, et al. Identification of an anti-inflammatory protein from Faecalibacterium prausnitzii, a commensal bacterium deficient in Crohn's disease. Gut 2016;65:415–425.

38. Abbeele P Van den, Belzer C, Goossens M, et al. Butyrate-producing Clostridium cluster XIVa species specifically colonize mucins in an in vitro gut model. ISME J 2013;7:949–961.

39. Duncan SH, Aminov RI, Scott KP, et al. Proposal of Roseburia faecis sp. nov., Roseburia hominis sp. nov. and Roseburia inulinivorans sp. nov., based on isolates from human faeces. Int J Syst Evol Microbiol 2006;56:2437–2441.

40. Khan MT, Duncan SH, Stams AJM, et al. The gut anaerobe Faecalibacterium prausnitzii uses an extracellular electron shuttle to grow at oxic-anoxic interphases. ISME J 2012;6:1578–1585.

41. **Elinav E, Strowig T**, Kau AL, et al. NLRP6 inflammasome regulates colonic microbial ecology and risk for colitis. Cell 2011;145:745–757.

42. Bloom SM, Bijanki VN, Nava GM, et al. Commensal Bacteroides species induce colitis in host-genotype-specific fashion in a mouse model of inflammatory bowel disease. Cell Host Microbe 2011;9:390–403.

43. Cash HL, Whitham CV, Hooper LV. Refolding, purification, and characterization of human and murine RegIII proteins expressed in Escherichia coli. Protein Expr Purif 2006;48:151–159.

44. Wirtz S, Popp V, Kindermann M, et al. Chemically induced mouse models of acute and chronic intestinal inflammation. Nat Protoc 2017;12:1295–1309.

45. Wehkamp J, Koslowski M, Wang G, et al. Barrier dysfunction due to distinct defensin deficiencies in small intestinal and colonic Crohn's disease. Mucosal Immunol 2008;1 Suppl 1:S67–74.

46. Ogawa H, Fukushima K, Naito H, et al. Increased expression of HIP/PAP and regenerating gene III in human inflammatory bowel disease and a murine bacterial reconstitution model. Inflamm Bowel Dis 2003;9:162–170.

Legends

Figure 1: hREG3A shapes gut microbiota in *REG3A*-transgenic mice. (*A*) Serum concentrations of human REG3A and murine Reg3g in wild-type (WT) and *REG3A*-transgenic mice (REG3A) before (Control) and after (Colitis) administration of DSS (n=6). (*B*) Digestive tract concentrations of hREG3A (n=3). (*C*) Colonic Reg3b and Reg3g mRNA expression level (n=5). (*D*) Alcian blue and anti-hREG3A stainings of colon tissue sections. Scale bar, 100µm. (*E*) PCA of bacterial profiles at the family level in the fecal microbiota of *REG3A*-transgenic (n=12) and WT (n=10) mice in the basal state. Each dot represents one mouse. P=0.001 (Monte-Carlo rank test). (*F*) Relative abundances of bacterial families in the basal state (Ctrl) of the same mouse cohorts as in (*E*) and on day 12 after onset of exposure to DSS (Colitis) in *REG3A*-transgenic (n=5) and WT (n=7) mice. (*G*) PCA of bacterial profiles at the family level in heterozygous (REG3A-TG+/-; n=15), homozygous (REG3A-TG+/+; n=12) and unrelated WT (n=11) mice of similar ages (Monte-Carlo rank test). Each dot represents one mouse. Yellow dots: WT dams of the REG3A-TG+/- mice (n=3). (*H*) Relative abundances of bacterial families in REG3A-TG+/- mice aged 9 and 12 weeks compared to WT (n=14) and to REG3A-TG+/+ mice. The data are averages ± SEM. Except for (*E*) and (*G*), the two-sided Wilcoxon rank sum test was performed for analysis. **P*<0.05, ***P*<0.01, ****P* <0.001.

Figure 2: hREG3A rescues bacteria from oxidative stress. (*A*) Ratio of Gram-positive to Gram-negative bacteria in the fecal microbiota of *REG3A*-transgenic (REG3A) and wild-type (WT) mice in the basal state (control) and on day 12 of induced colitis. Same cohorts as in Figure 1*E* and *F*. (*B*) Bacterial ROS levels in the fecal microbiota of REG3A and WT mice (n=6 per group) measured by flow cytometry and H_2-DCFDA during the period of DSS administration. *P*=0.019 (two-way ANOVA). (*C*) Growth of Gram-positive *Enterococcus*

faecalis under oxidative stress. PQT: paraquat. CFU: colony forming units. rcREG3A: recombinant human REG3A protein. Assays were done in quadruplicate in 3 independent experiments. (*D*) Cellular ROS levels in *E. faecalis* cultures measured by flow cytometry with H_2-DCFDA. Left: Representative flow cytometry curves. H_2-DCFDA high cells: the 15% most strongly fluorescent cells in the PQT+buffer condition. Right: Percentage of bacteria in the high-intensity range in 3 independent experiments. (*E*) Cell viability by flow cytometry with propidium iodide (PI). Normalized CFU numbers of Gram-positive *Roseburia intestinalis* and *Faecalibacterium prausnitzii* in strictly anaerobic cultures (*F*) and after exposure to ambient air (*G*). The numbers of CFUs were normalized to the average CFU number measured in control cultures (buffer). Assays were done in quadruplicate in two independent experiments. The data are averages ± SEM. The two-sided Wilcoxon rank sum test was performed for analysis except for (*B*). **P*<0.05, ****P* <0.001.

Figure 3: *REG3A*-transgenic mice have a lower susceptibility to DSS-induced colitis than WT mice. (*A-D*) Time evolution of DSS-induced colitis in *REG3A*-transgenic (REG3A) and wild-type (WT) mice (n=20 for each group; 2 independent experiments). Heavy line: 5-day period of DSS administration. (*A*) Body weight change. (*B*) Rectal bleeding score. (*C*) Diarrhea score. (*D*) Kaplan-Meier survival plot. (*E*) Representative day-12 colon images stained with hematoxylin, eosin and alcian blue. Scale bar, 50µm. (*F*) Histological assessment of gut epithelium (n=14 for each group). (*G*) Representative whole-body [^{18}F]FDG PET images. The images are frontal slices of 3D volumes passing through heart. H: heart. B: bladder. C: colon. *: Absence of colon uptake. (*H*) Quantification of [^{18}F]FDG over time (n=3). *P*=0.013 (two-way ANOVA). (*I*) mRNA expression level of the indicated inflammatory markers in colonic epithelial cells of WT and *REG3A*-transgenic mice (n=5).

The data are means ± SEM. The two-sided Wilcoxon rank sum test was performed for analysis except for (*H*). **P* <0.05, ***P* <0.01, ****P* <0.001.

Figure 4: Gut barrier integrity and weak inflammation in *REG3A*-transgenic mice exposed to DSS or TNBS. (*A-G*) Mice exposed to DSS. (*A*) Anti-MUC2 mucin immunofluorescence, bacterial 16S rRNA FISH and DAPI images of colon tissues from WT and *REG3A*-transgenic mice on day 12 of DSS-induced colitis. Scale bars, 20µm. (*B*) Representative anti-Wheat Germ Agglutinin immunoblots (IB WGA) at the indicated time points of DSS-induced colitis. Bar chart: densitometric analysis (n=5 for each group; 2 independent experiments). (*C*) Bacterial translocation in mesenteric lymph nodes before (n=4) and during colitis (n=5). (*D*) Changes in expression level of the genes related to the lipopolysaccharide (LPS)-induced activation pathway that were the most downregulated in *REG3A*-transgenic mice. (*E*) Serum levels of LPS (n=8). (*F*) Serum levels of soluble CD14 (n=8). (*G*) Concentration of malondialdehyde (MDA) in gut epithelium extracts (n=9-14). (*H-J*) Mice exposed to TNBS. *REG3A*-transgenic and WT mice were administered TNBS together with ethanol intrarectally (n=15 per group). (*H*) Ameho quantitative histological score and two representative histological examinations for each group two days after TNBS administration. Scale bar, 100µm. (*I*) mRNA expression level of the *Il1b* and *Tnf* inflammatory cytokines. (*J*) Myeloperoxidase (MPO) concentration in colon tissue extracts. The data are represented either as box plots or means ± SEM. The two-sided Wilcoxon rank sum test was performed for analysis. **P* <0.05, ***P* <0.01, ****P* <0.001.

Figure 5: Alleviated colitis severity in conventional and germ-free mice colonized with a hREG3A-shaped microbiota. (*A*) Relative abundances of bacterial families in the fecal microbiota of WT mice cohoused with *REG3A*-transgenic mice for 8 weeks (CoH WT; n=8)

compared to single-housed WT (n=10) and *REG3A*-transgenic (n=7) mice. (*B-E*) Time evolution of DSS-induced colitis in cohoused WT and single-housed WT mice. Heavy line: 5-day period of DSS administration. (*B*) Body weight change. (*C*) Rectal bleeding score. (*D*) Diarrhea score. (*E*) Kaplan-Meier survival plot (p=ns). (*G*) Histological assessment of gut epithelium (n=5). (*H*) PCA at the family level of germ-free mice colonized with microbiota from WT (ExGF-WT; n=8) and *REG3A*-transgenic (ExGF-TG; n=8) mice 3 weeks after mice were fed feces (day 0). inoc: inoculum used for oral gavage. P=0.001 (Monte-Carlo rank test). (*I*) Relative abundances of the main bacterial families that are overrepresented in conventional *REG3A*-transgenic mice at day 0. (*J-M*) Time evolution of DSS-induced colitis in ExGF-WT and ExGF-TG mice. Heavy line: 5-day period of DSS administration. (*J*) Body weight change. (*K*) Rectal bleeding score. (*L*) Diarrhea score. (*M*) Kaplan-Meier survival plot. (*N*) Gene enrichment of TLR4 pathway on day 12 of colitis. NES: normalized enrichment score. (*O*) Serum LPS levels. (*P*) mRNA expression level of the indicated pro- and anti-inflammatory markers in colonic epithelial cells of ExGF-WT and ExGF-TG mice (n=5). The data are averages ± SEM. Except in (*H*), the two-sided Wilcoxon rank sum test was performed for analysis. **P*<0.05, ***P*<0.01, ****P* <0.001.

Figure 6: Intrarectal administration of hREG3A decreased colon damage and inflammation in WT mice with colitis. 100µg of a recombinant REG3A protein (rcREG3A; n=14) or an equivalent volume of buffer (n=15) was administered intrarectally in WT mice with colitis on the day before (D0) and on the day (D1) of TNBS administration. (*A*) Body weight change. (*B*) Ameho quantitative histological score and representative colon images stained with hematoxylin and eosin. Scale bar, 100µm. (*C*) Colonic mRNA expression level of *Il1b* and *Tnf*. (*D*) Myeloperoxidase (MPO) in colon tissue extracts. The data are averages ± SEM. The two-sided Wilcoxon rank sum test was performed for analysis. **P*<0.05, ***P*<0.01, ****P* <0.001.

Figure1

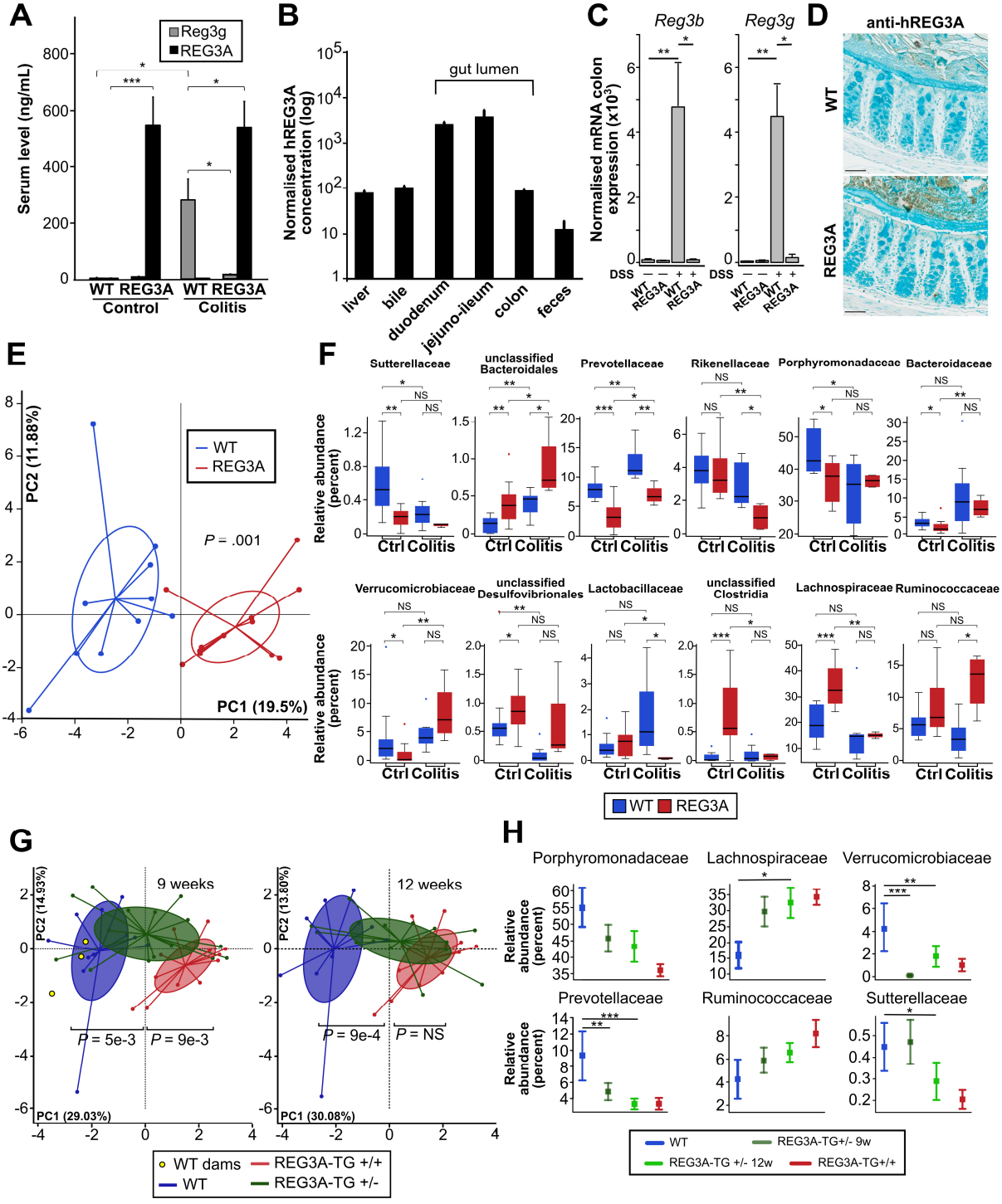
A
Reg3g
REG3A
Serum level (ng/mL)
WT REG3A WT REG3A
Control Colitis
B
Normalised hREG3A concentration (log)
gut lumen
liver
bile
duodenum
jejuno-ileum
colon
feces
C
Reg3b
Reg3g
Normalised mRNA colon expression (x10^3)
DSS
WT REG3A WT REG3A
D
anti-hREG3A
WT
REG3A
E
PC2 (11.88%)
PC1 (19.5%)
WT
REG3A
P = .001
F
Sutterellaceae
unclassified Bacteroidales
Prevotellaceae
Rikenellaceae
Porphyromonadaceae
Bacteroidaceae
Verrucomicrobiaceae
unclassified Desulfovibrionales
Lactobacillaceae
unclassified Clostridia
Lachnospiraceae
Ruminococcaceae
Relative abundance (percent)
Ctrl Colitis
WT REG3A
G
9 weeks
12 weeks
PC2 (14.93%)
PC1 (29.03%)
PC2 (13.80%)
PC1 (30.08%)
P = 5e-3
P = 9e-3
P = 9e-4
P = NS
WT dams
WT
REG3A-TG +/+
REG3A-TG +/-
H
Porphyromonadaceae
Lachnospiraceae
Verrucomicrobiaceae
Prevotellaceae
Ruminococcaceae
Sutterellaceae
Relative abundance (percent)
WT
REG3A-TG+/- 9w
REG3A-TG +/- 12w
REG3A-TG+/+

Figure 2

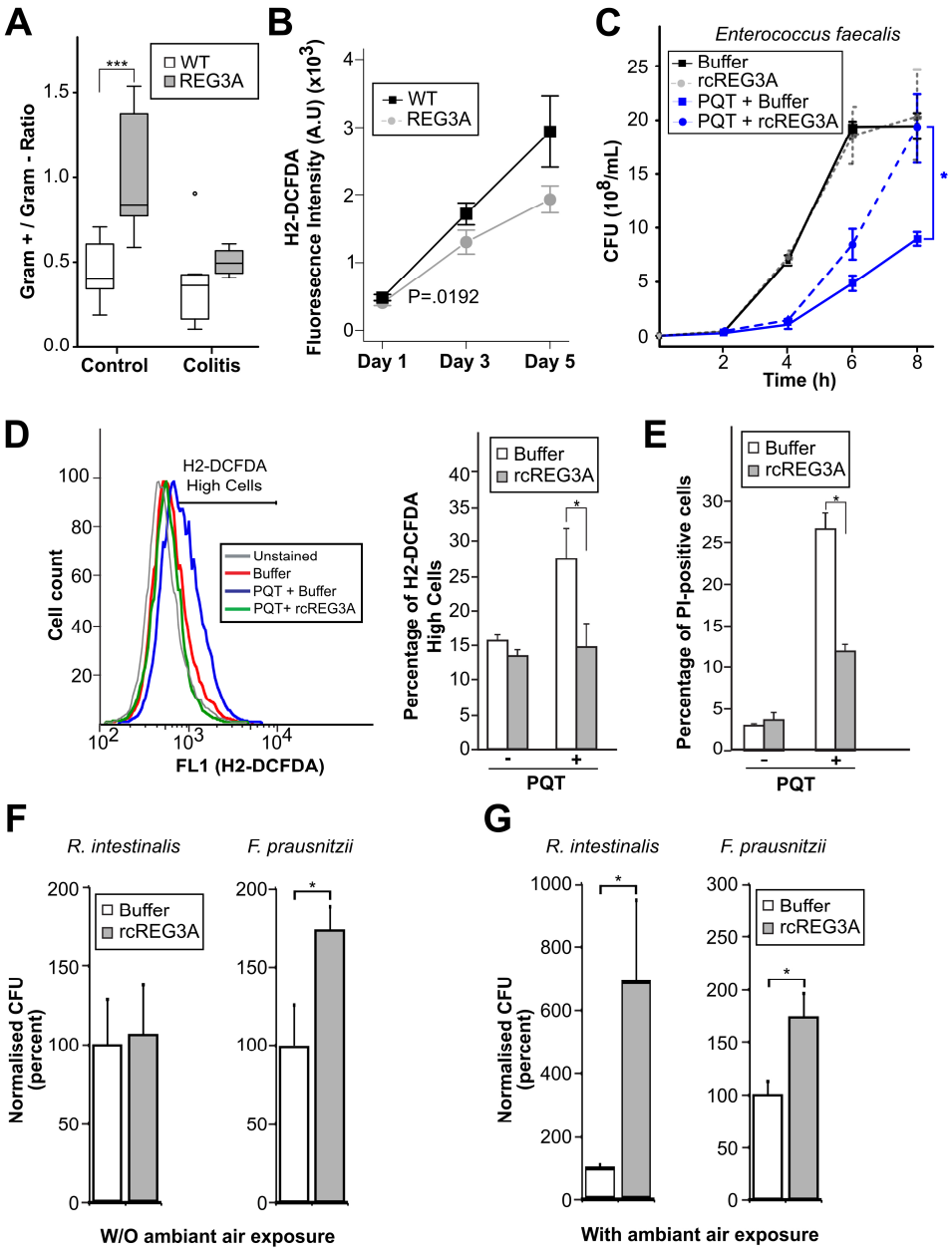
A
Gram + / Gram - Ratio
WT
REG3A
***
Control
Colitis
B
H2-DCFDA Fluoresecnce Intensity (A.U) (x10^3)
WT
REG3A
P=.0192
Day 1
Day 3
Day 5
C
Enterococcus faecalis
CFU (10^8/mL)
Buffer
rcREG3A
PQT + Buffer
PQT + rcREG3A
Time (h)
D
H2-DCFDA
High Cells
Cell count
Unstained
Buffer
PQT + Buffer
PQT+ rcREG3A
FL1 (H2-DCFDA)
Percentage of H2-DCFDA High Cells
Buffer
rcREG3A
PQT
E
Percentage of PI-positive cells
Buffer
rcREG3A
PQT
F
R. intestinalis
F. prausnitzii
Normalised CFU (percent)
Buffer
rcREG3A
W/O ambiant air exposure
G
R. intestinalis
F. prausnitzii
Normalised CFU (percent)
Buffer
rcREG3A
With ambiant air exposure

Figure 3

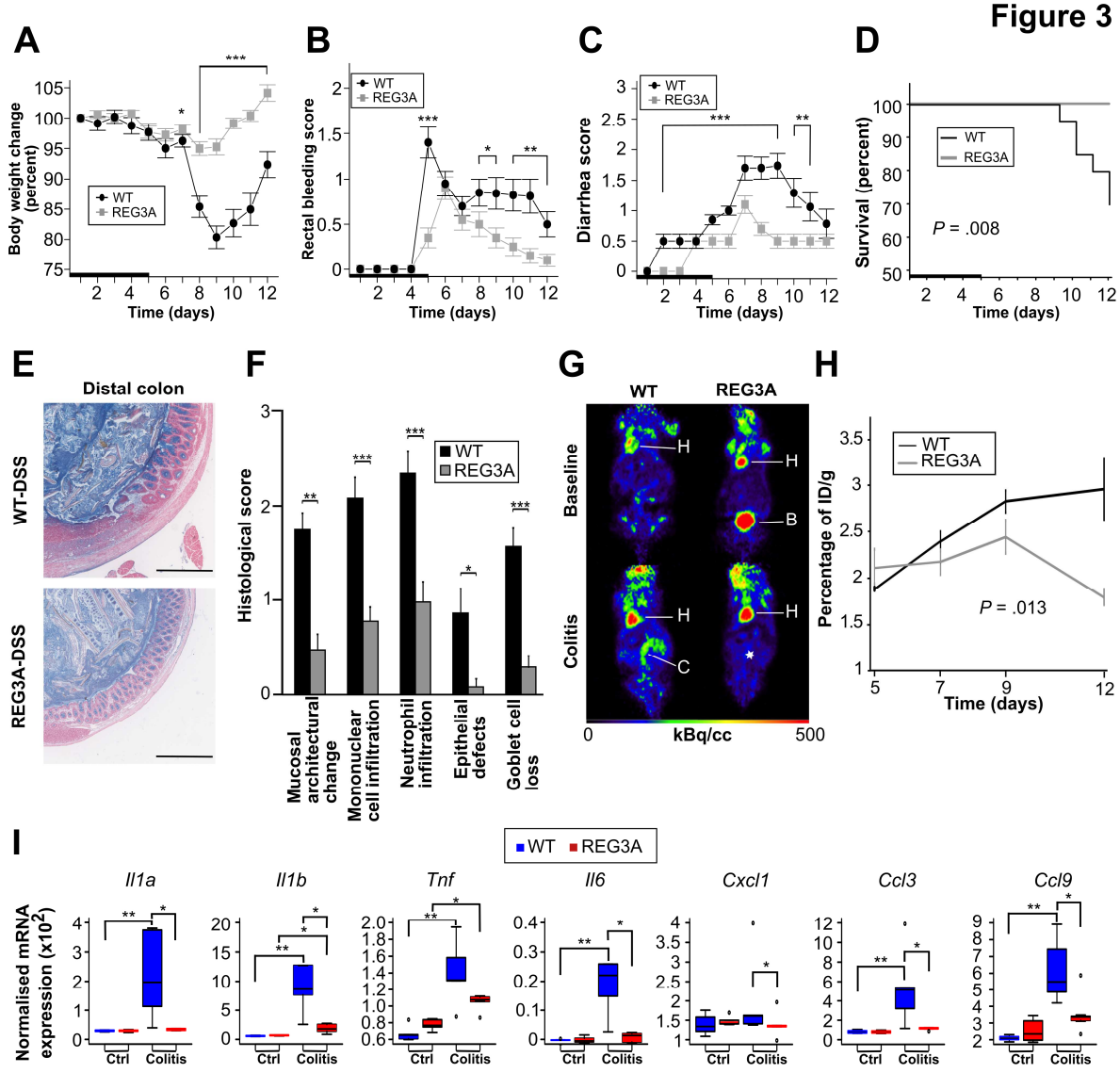
A
Body weight change (percent)
Time (days)
WT
REG3A
B
Rectal bleeding score
Time (days)
C
Diarrhea score
Time (days)
D
Survival (percent)
P = .008
Time (days)
E
Distal colon
WT-DSS
REG3A-DSS
F
Histological score
Mucosal architectural change
Mononuclear cell infiltration
Neutrophil infiltration
Epithelial defects
Goblet cell loss
G
WT
REG3A
Baseline
Colitis
kBq/cc
H
Percentage of ID/g
P = .013
Time (days)
I
Il1a
Il1b
Tnf
Il6
Cxcl1
Ccl3
Ccl9
Normalised mRNA expression (x10²)
Ctrl
Colitis

Figure 4

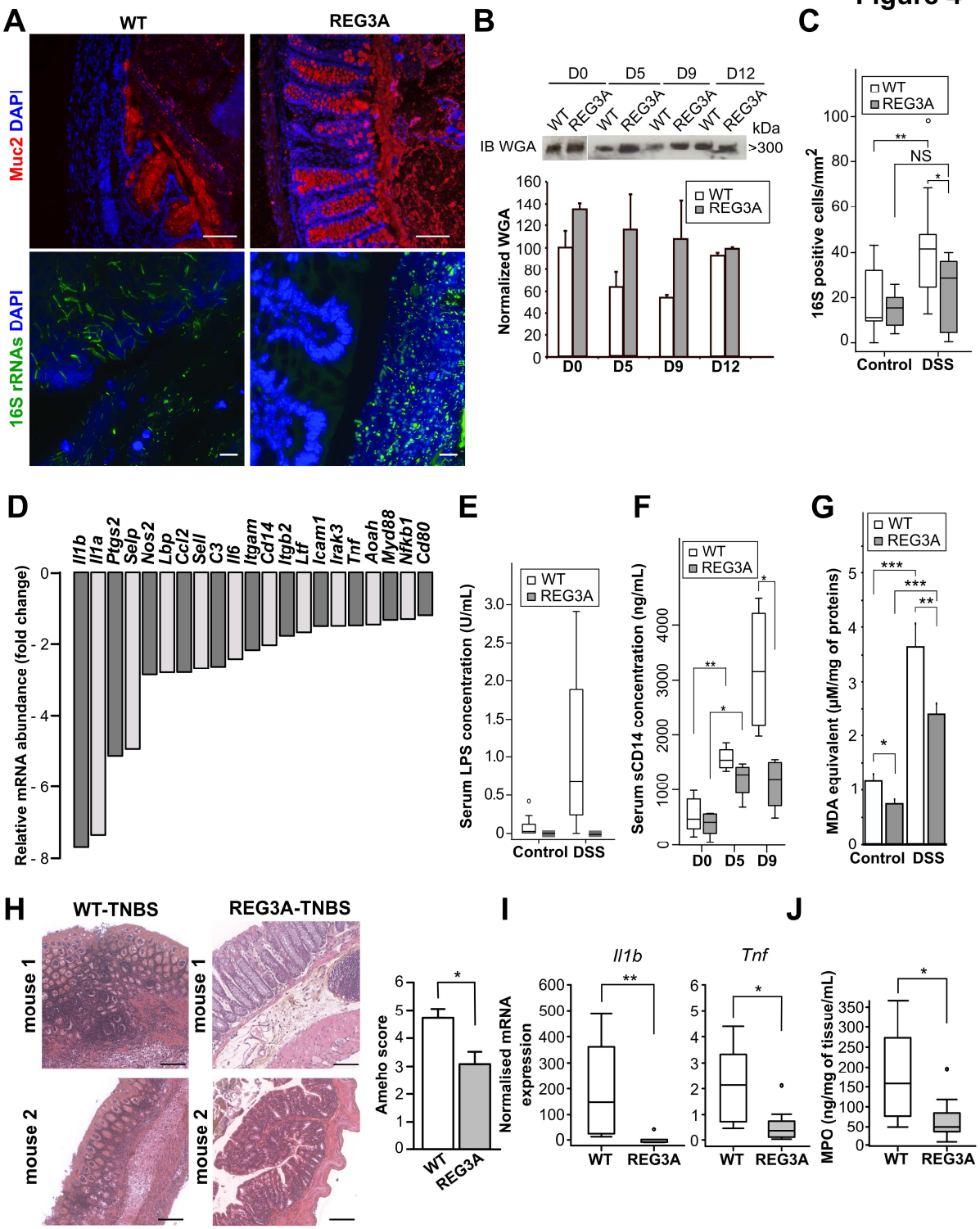
A
WT
REG3A
Muc2 DAPI
16S rRNAs DAPI
B
D0
D5
D9
D12
WT
REG3A
kDa
IB WGA
>300
Normalized WGA
C
16S positive cells/mm2
Control
DSS
NS
D
Relative mRNA abundance (fold change)
Il1b
Il1a
Ptgs2
Selp
Nos2
Lbp
Ccl2
Sell
C3
Il6
Itgam
Cd14
Itgb2
Ltf
Icam1
Irak3
Tnf
Aoah
Myd88
Nfkb1
Cd80
E
Serum LPS concentration (U/mL)
F
Serum sCD14 concentration (ng/mL)
G
MDA equivalent (μM/mg of proteins)
H
WT-TNBS
REG3A-TNBS
mouse 1
mouse 2
Ameho score
I
Il1b
Tnf
Normalised mRNA expression
J
MPO (ng/mg of tissue/mL)

Figure 5

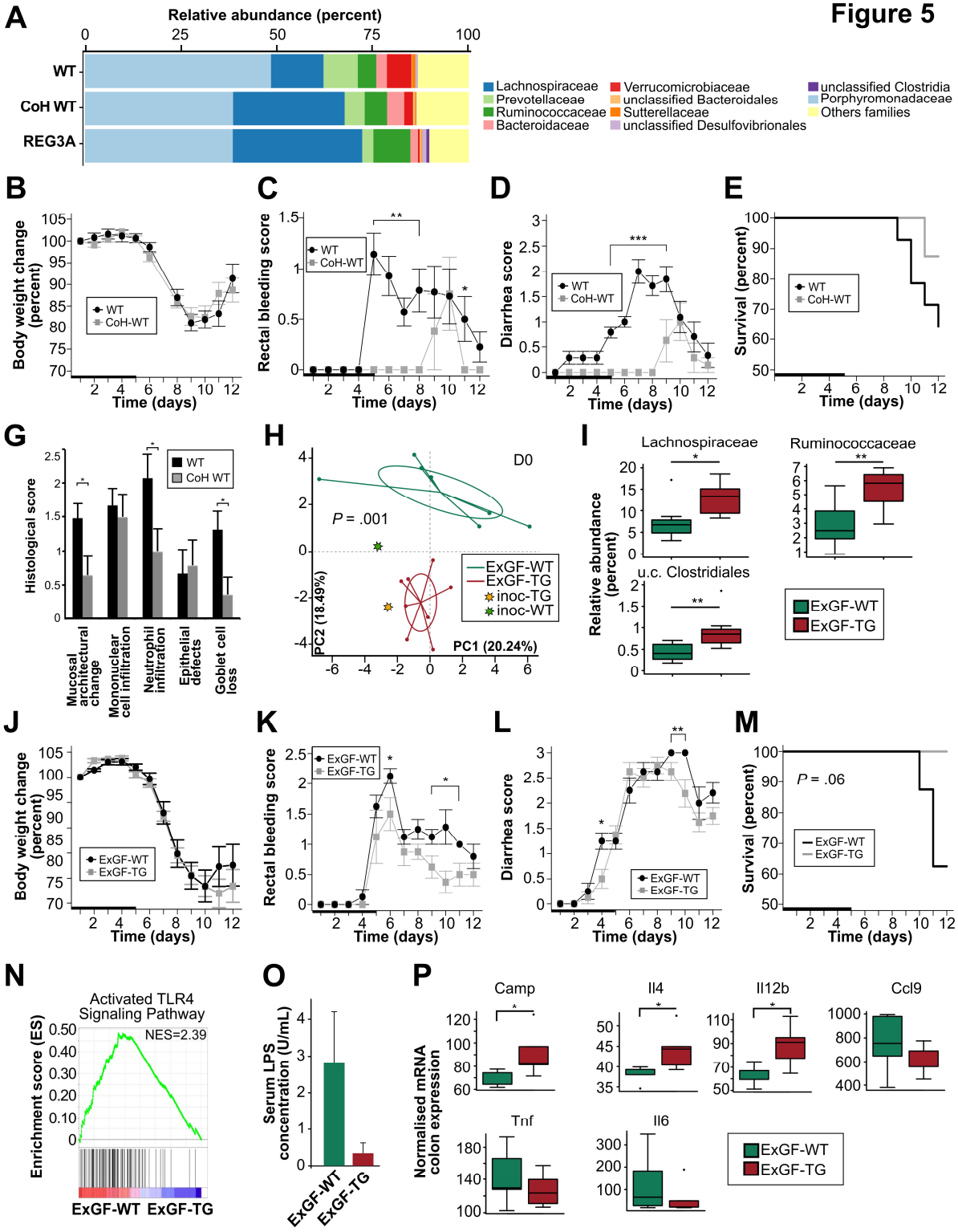
A
Relative abundance (percent)
WT
CoH WT
REG3A
Lachnospiraceae
Prevotellaceae
Ruminococcaceae
Bacteroidaceae
Verrucomicrobiaceae
unclassified Bacteroidales
Sutterellaceae
unclassified Desulfovibrionales
unclassified Clostridia
Porphyromonadaceae
Others families
B
Body weight change (percent)
Time (days)
C
Rectal bleeding score
D
Diarrhea score
E
Survival (percent)
G
Histological score
Mucosal architectural change
Mononuclear cell infiltration
Neutrophil infiltration
Epithelial defects
Goblet cell loss
H
D0
P = .001
PC1 (20.49%)
PC2 (18.49%)
ExGF-WT
ExGF-TG
inoc-TG
inoc-WT
I
Lachnospiraceae
Ruminococcaceae
u.c. Clostridiales
Relative abundance (percent)
J
K
L
M
P = .06
N
Activated TLR4 Signaling Pathway
NES=2.39
Enrichment score (ES)
O
Serum LPS concentration (U/mL)
P
Camp
Il4
Il12b
Ccl9
Tnf
Il6
Normalised mRNA colon expression

Figure 6

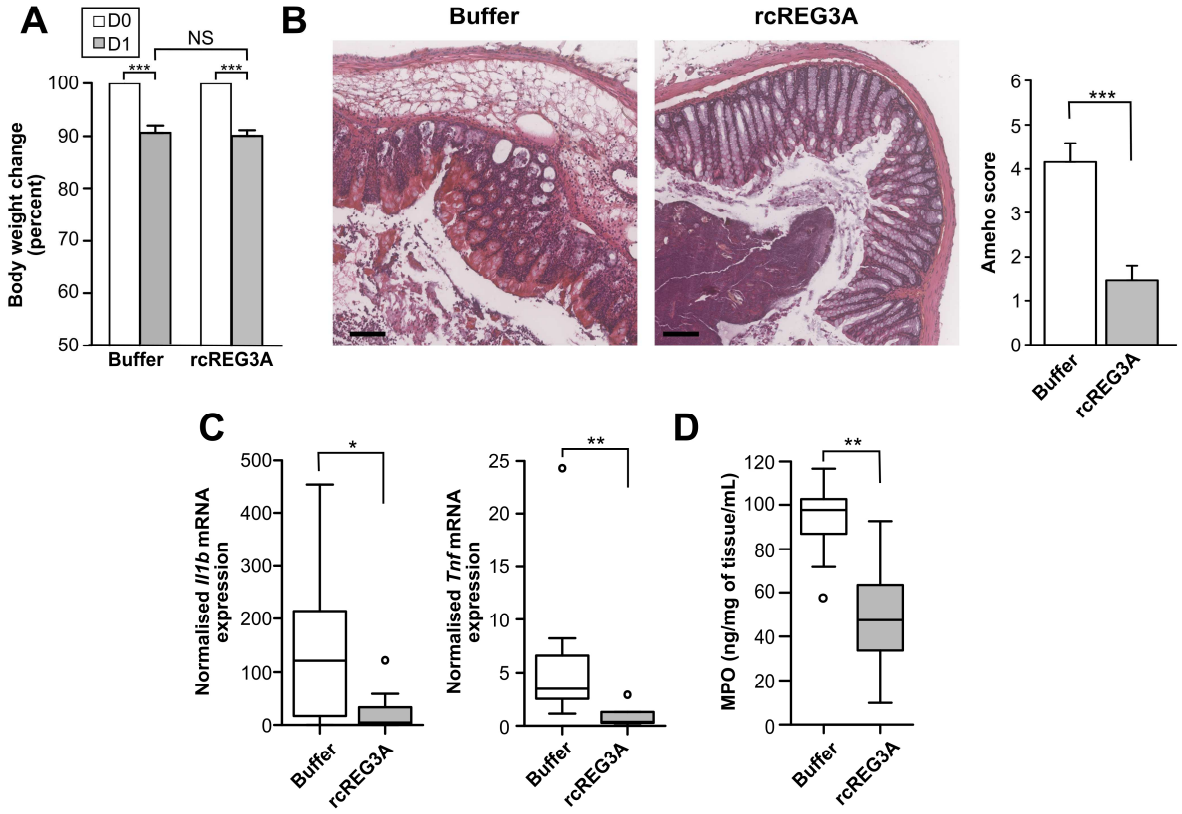
A
D0
D1
NS
***
***
Body weight change (percent)
100
90
80
70
60
50
Buffer
rcREG3A
B
Buffer
rcREG3A
Ameho score
6
5
4
3
2
1
0
***
Buffer
rcREG3A
C
Normalised Il1b mRNA expression
500
400
300
200
100
0
*
Buffer
rcREG3A
Normalised Tnf mRNA expression
25
20
15
10
5
0
**
Buffer
rcREG3A
D
MPO (ng/mg of tissue/mL)
120
100
80
60
40
20
0
**
Buffer
rcREG3A

Supplementary Figure S1

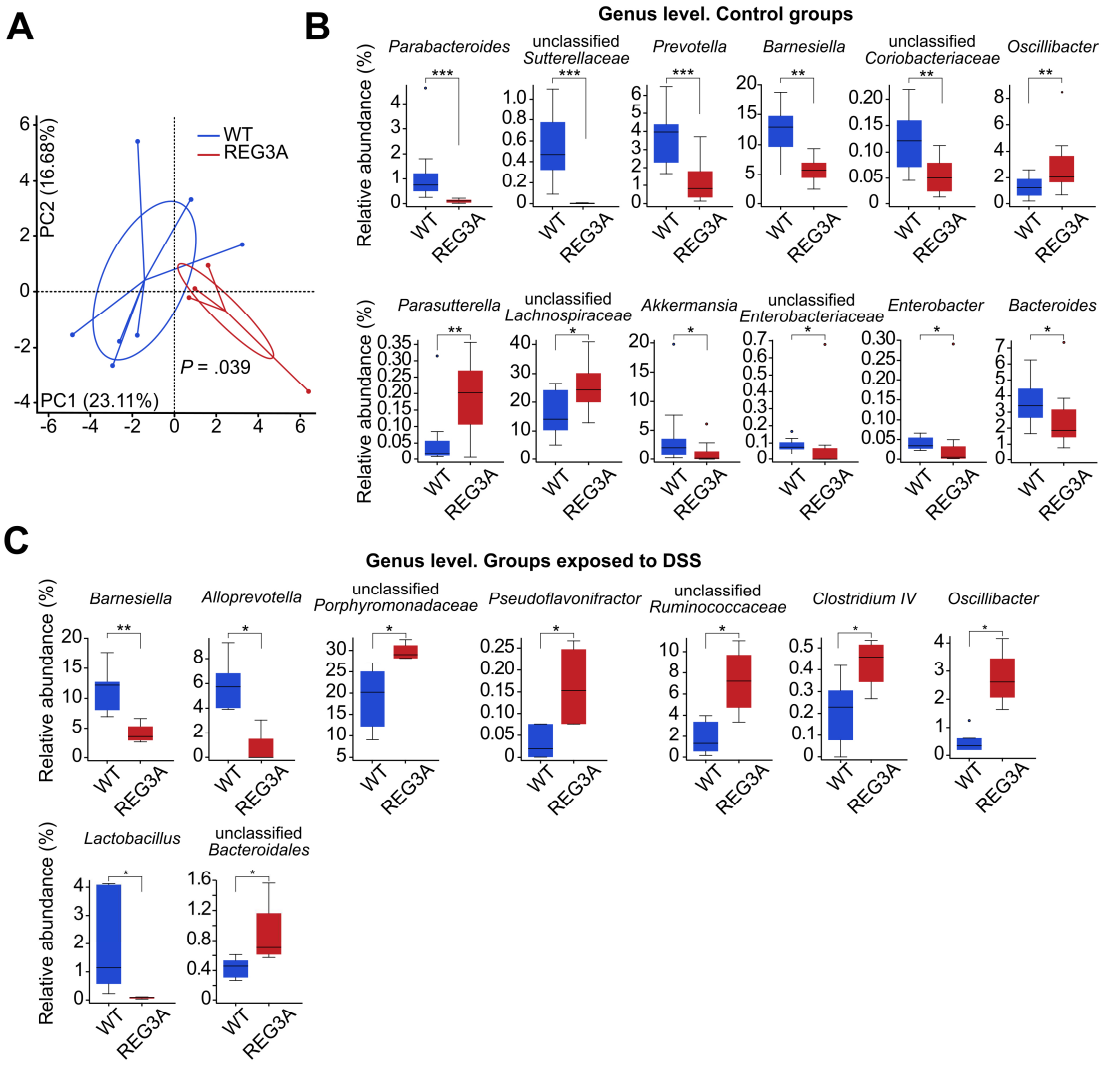

Supplementary Figure S2

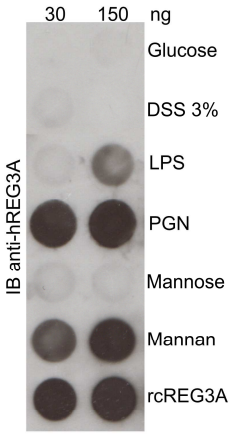

Supplementary Figure S3

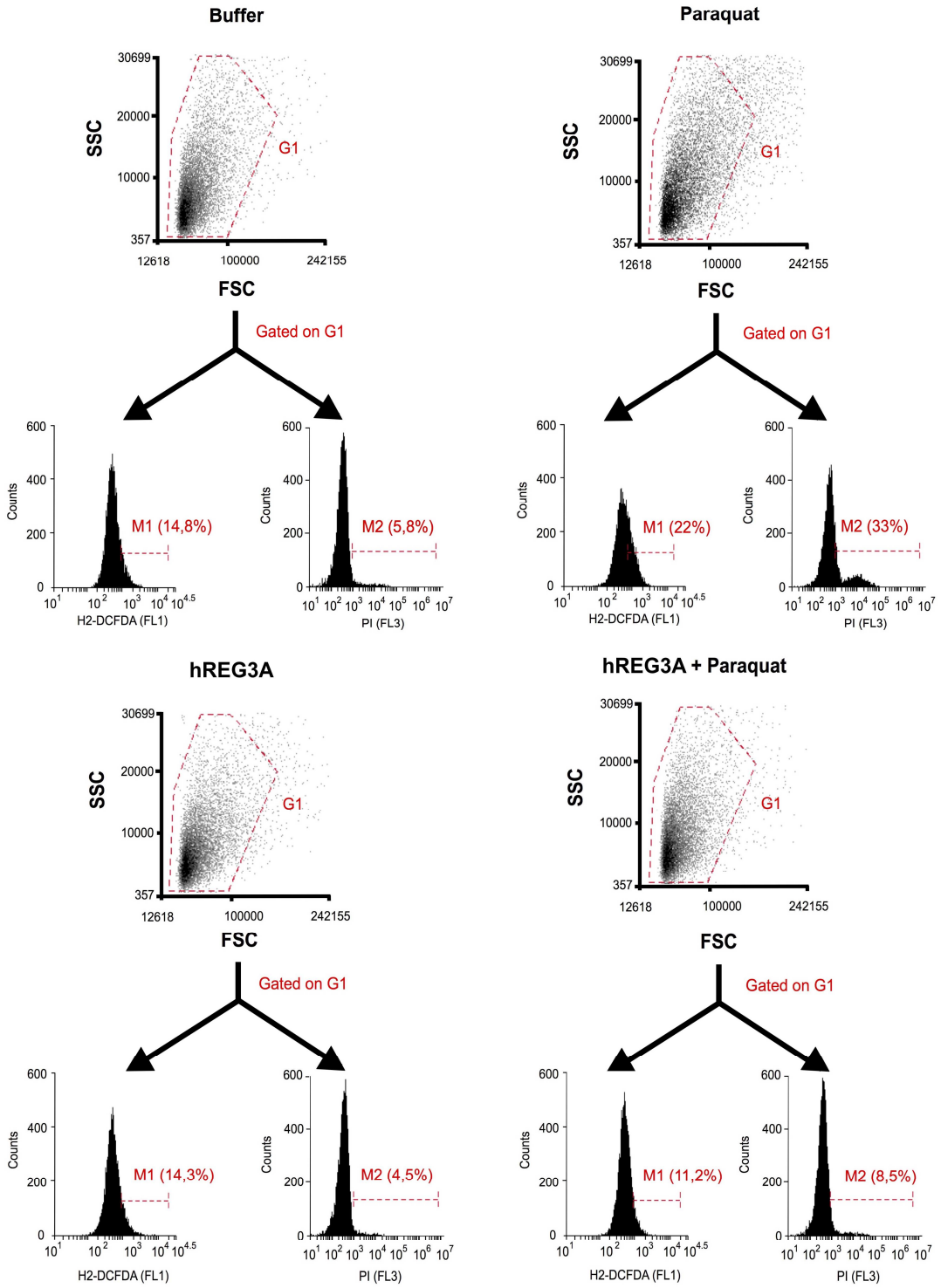

Supplementary Figure S4

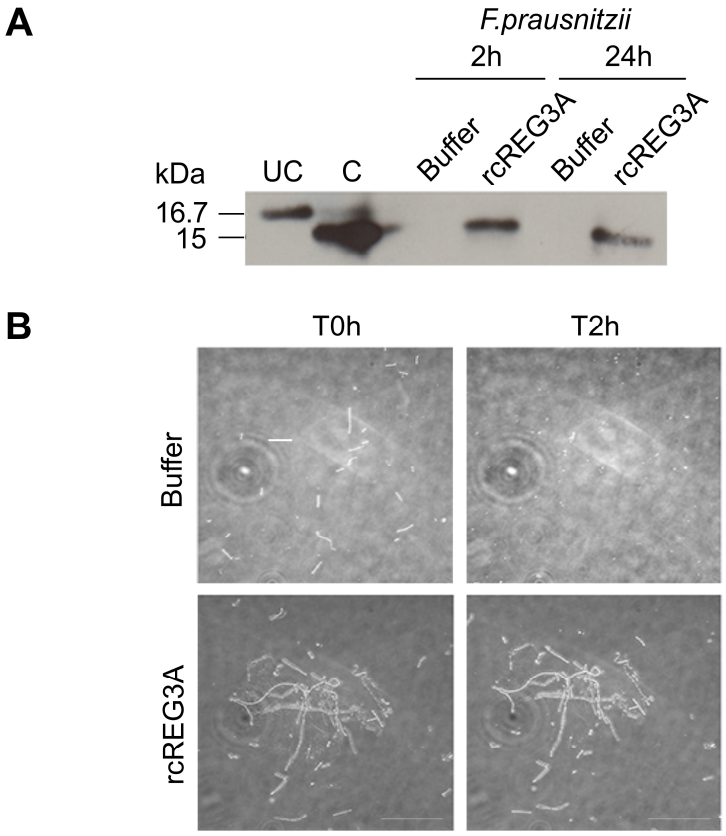

Supplementary Figure S5

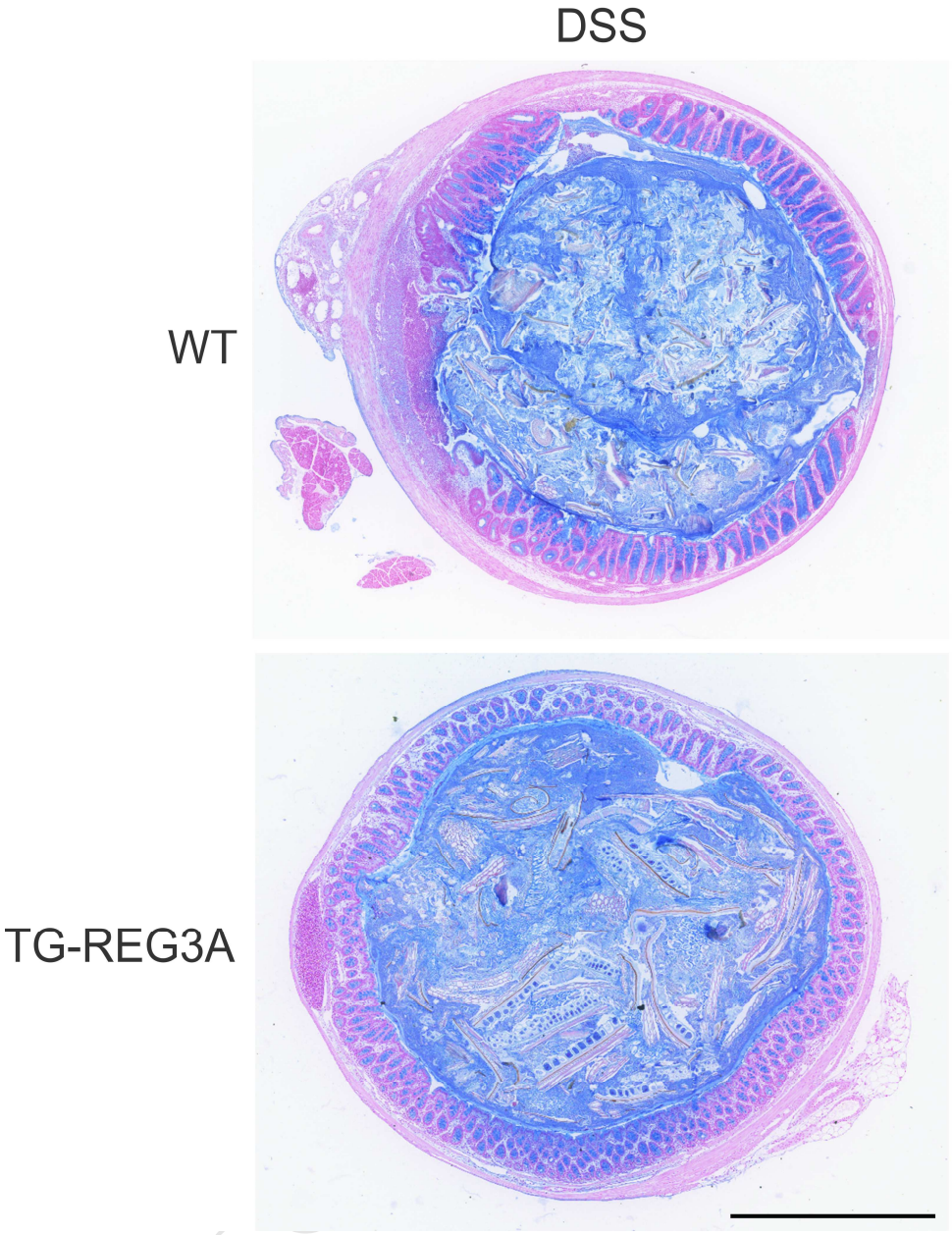

Supplementary Figure S6

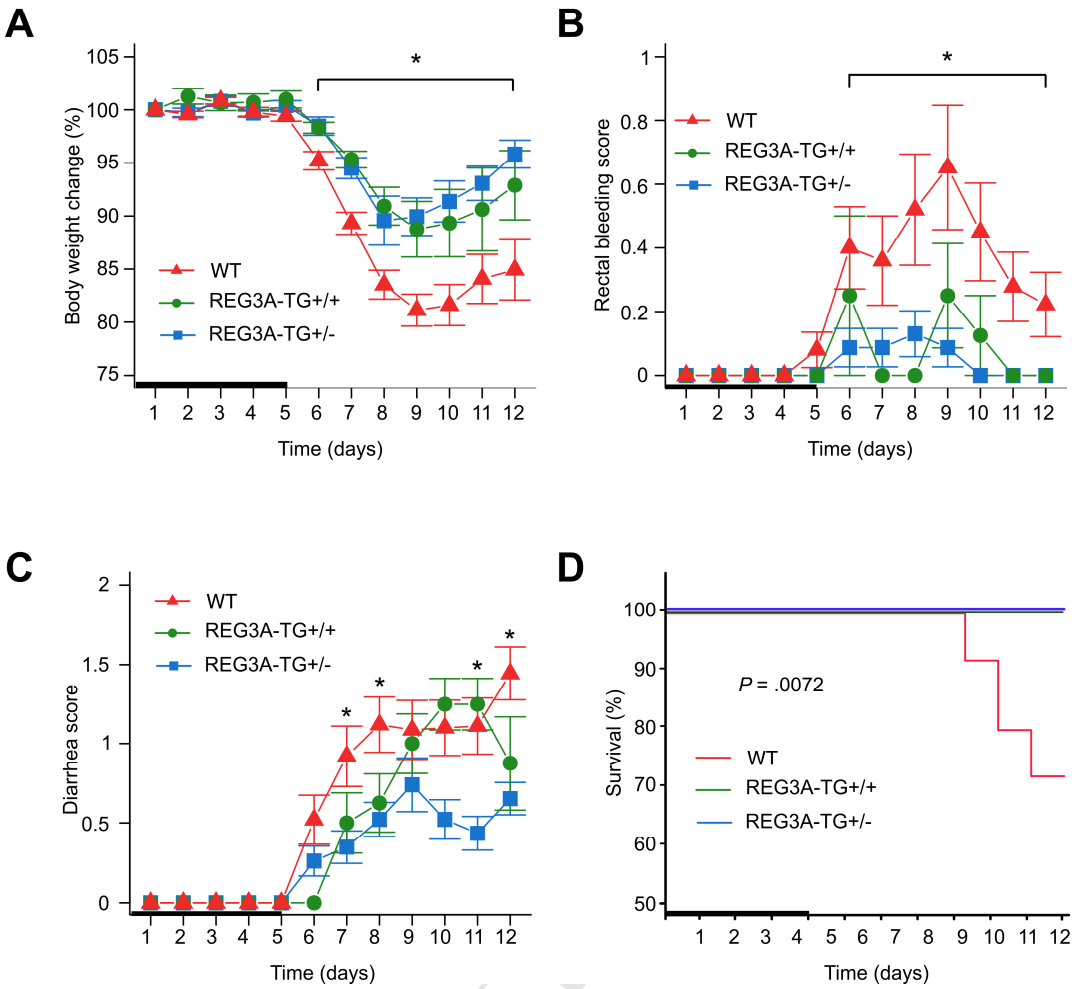

Supplementary Figure S7

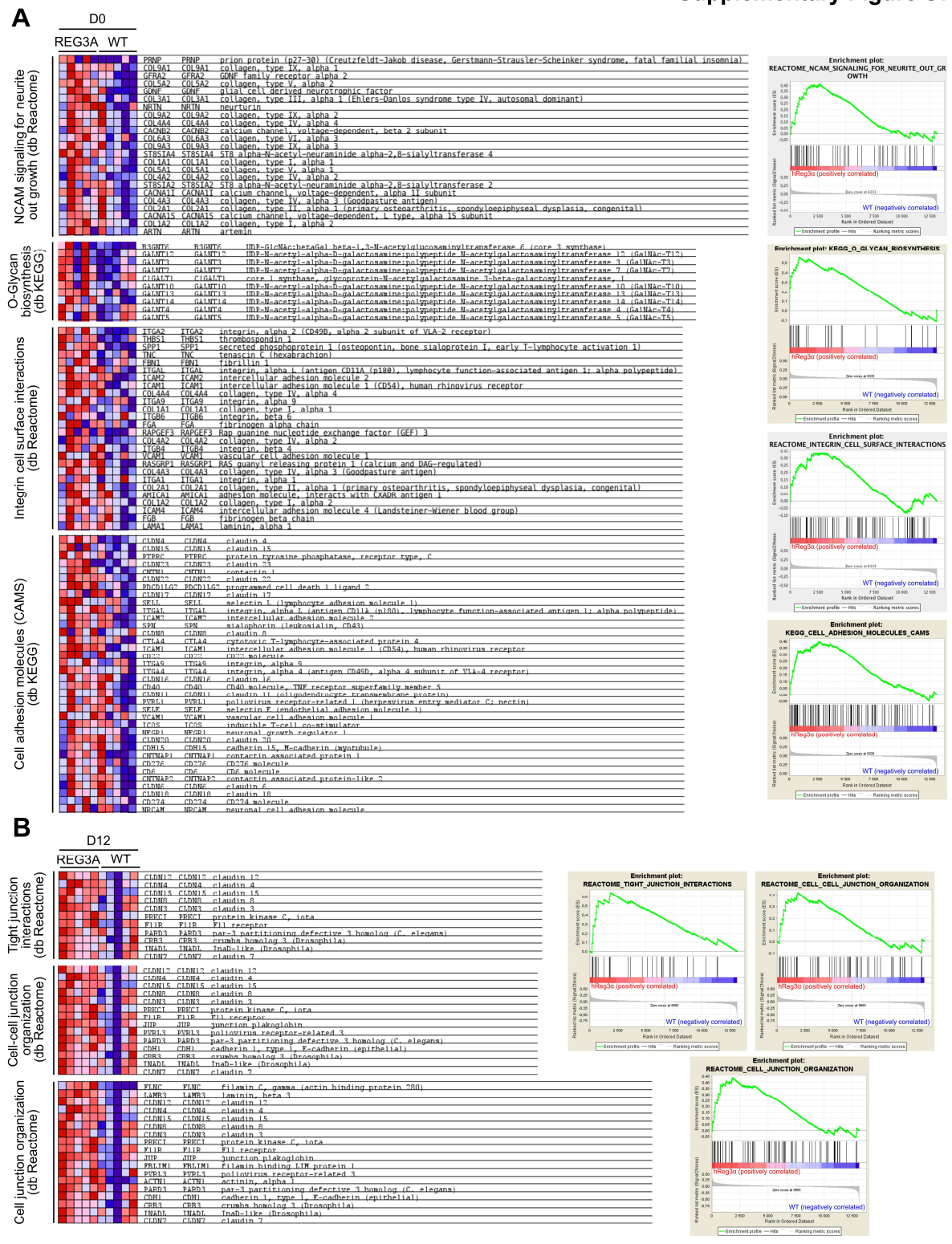

Supplementary Figure S8

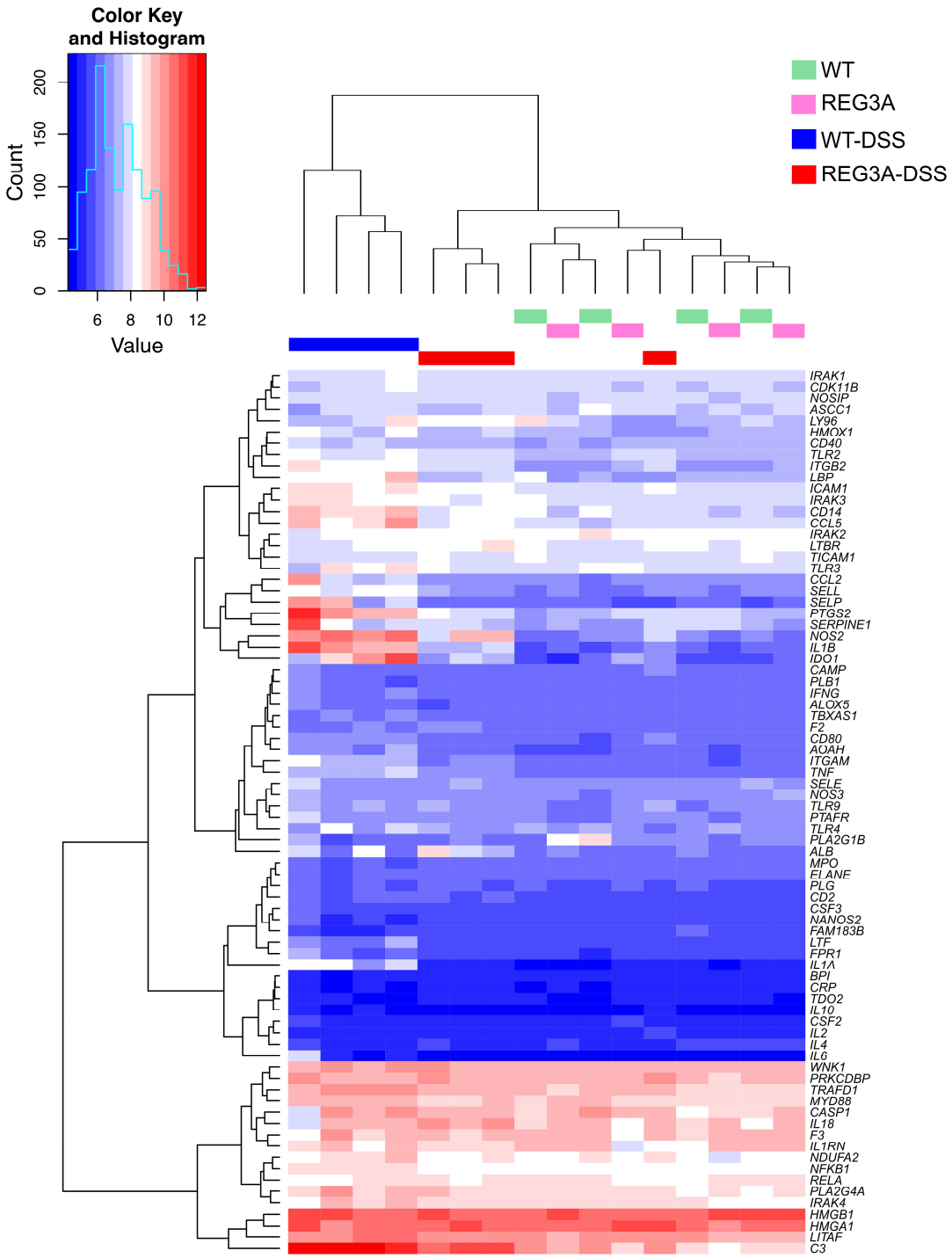

Supplementary Figure S9

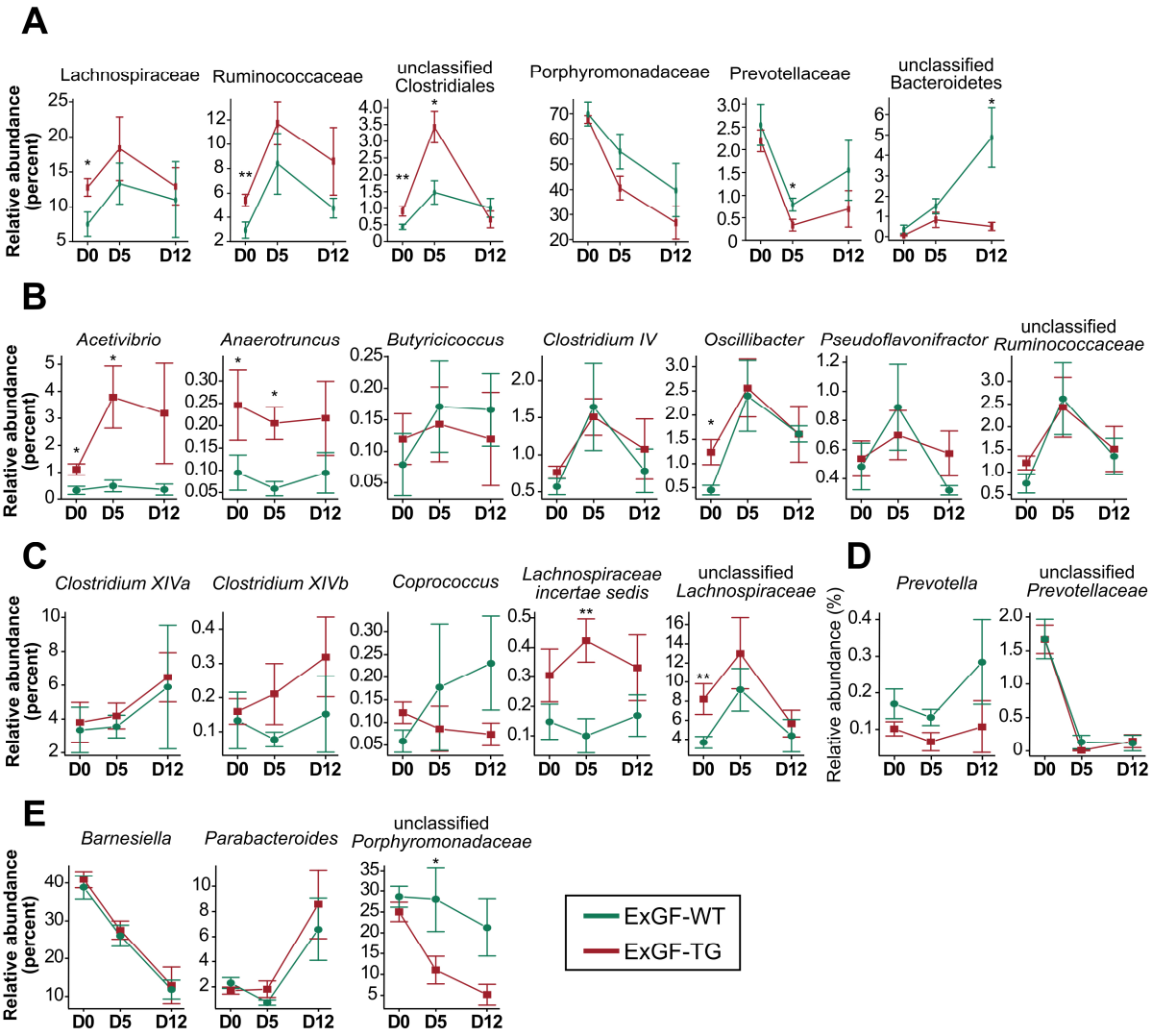

Supplementary Figure S10

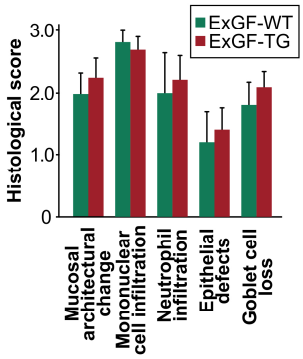

Supplementary Figure S11

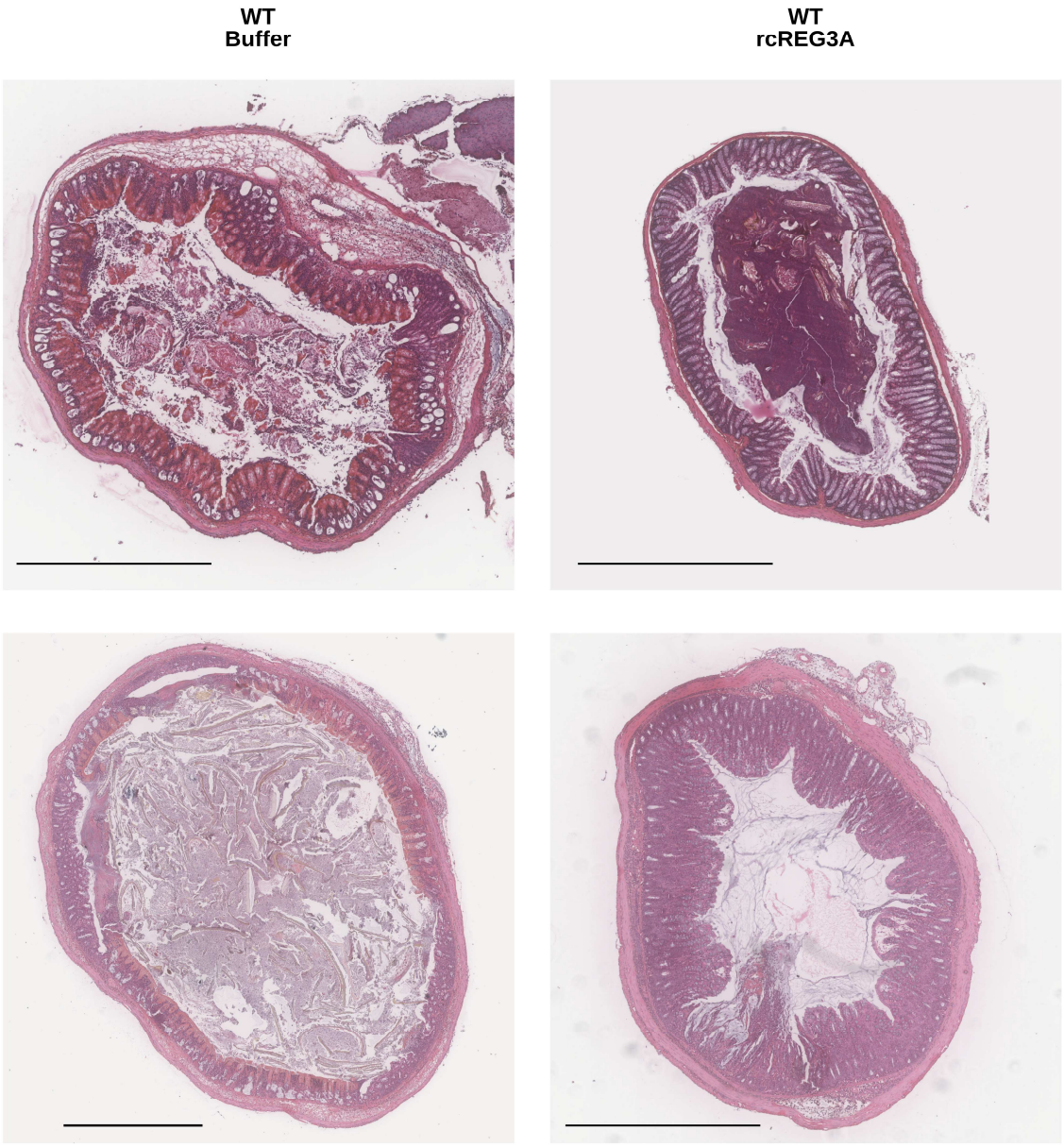

Legends to Supplemental Figures

Figure S1: Gut microbiota composition under homeostatic and inflammatory conditions in *REG3A*-transgenic mice. (*A*) PCA plots of bacterial profiles at the family level in *REG3A*-transgenic (n=4) and WT (n=7) mice on day 12 of induced colitis. P=0.039 (Monte-Carlo rank test). Each dot represents one mouse. (*B*) and (*C*) Relative abundances of bacterial genera in (*B*) the homeostatic (Control groups) and (*C*) inflammatory (Groups exposed to DSS) states. The data are averages ± SEM. The Wilcoxon rank-sum test was performed for analysis.

Figure S2: The hREG3A lectin does not interact with dextran sodium sulphate. Dot blot of hREG3A binding to the indicated immobilized mono- and polysaccharides followed by anti-hREG3A immunoblotting (IB). DSS: dextran sodium sulphate. LPS: lipopolysaccharides. PGN: peptidoglycans. rcREG3A: recombinant REG3A protein. The lane labeled rcREG3A received no saccharides.

Figure S3: Representative flow cytometry plots of cellular ROS levels (H_2-DCFDA dye; FL1 detector) and cell viability (PI; FL3 detector) in *E. faecalis* cultures exposed to Paraquat and hREG3A. Gate G1 (alive cell population) representing 90% of the total cell population was defined in the forward (FSC) and side (SSC) scatter light plots in the cultures incubated with buffer. Gate M1 was set to include the 15% most strongly FL1 fluorescent cells and Gate M2 the 5% most strongly FL3 fluorescent cells in the buffer condition. The same G1, M1 and M2 gates were used in the analysis of cultures exposed to Paraquat and hREG3A.

Figure S4: **hREG3A increases the viability of *Faecalibacterium prausnitzii* exposed to ambient air.** (*A*) Anti-hREG3A immunoblot from *F. prausnitzii* anaerobic cultures incubated with a recombinant human REG3A protein (rcREG3A) for 2h or 24h. Uncleaved (UC) and cleaved (C) rcREG3A: control signals. (*B*) Micrographs of slide-mounted *F. prausnitzii* colonies without or with rcREG3A before (T0h) and after (T2h) exposure to ambient air. Scale bar, 20µm.

Figure S5: Representative colon images stained with hematoxylin, eosin and alcian blue at day 12 of DSS-induced colitis in *REG3A*-transgenic (TG-REG3A) and WT mice. Same colon sections as in Figure 3*E*. Scale bar, 1mm.

Figure S6: Low susceptibility to induced colitis of *REG3A* heterozygous mice born to WT mothers compared to WT mice. (*A-D*) Time evolution of DSS-induced colitis in *REG3A* heterozygous (REG3A-TG+/-; n=15), *REG3A* homozygous (REG3A-TG+/+; n=12) and wild-type (WT; n=15) mice. (*A*) Body weight changes. (*B*) Rectal bleeding score. (*C*) Diarrhea score. (*D*) Kaplan-Meier survival plot. Heavy line: 5-day period of DSS administration. The data are means ± SEM. The Wilcoxon rank-sum test was performed for analysis. ***P* <0.01, ****P* <0.001.

Figure S7: **Transcriptomic profiles of gene sets involved in the regulation of the gut barrier function.** (*A*) and (*B*) Enrichment plots of genes related to gut barrier function and the corresponding heat maps for *REG3A*-transgenic and WT mice. (*A*) Homeostatic state (D0). (*B*) At day 12 of DSS-induced colitis (D12). *P*<0.001 for all the indicated pathways (empirical phenotype-based permutation test).

Figure S8: Attenuation of the lipopolysaccharide (LPS) activation pathway in the colon of *REG3A*-transgenic mice exposed to DSS. Hierarchical clustering for genes related to the LPS-induced activation pathway in healthy and DSS-given *REG3A*-transgenic and WT mice (n=4 per group).

Figure S9: Time evolution of bacterial communities in colonized germ-free mice during DSS-induced colitis. (*A*-*E*) Relative abundances of bacterial communities in germ-free mice colonized with the faecal microbiota from *REG3A*-transgenic (ExGF-TG; n=8) and WT mice (ExGF-WT; n=8) on days 0, 5 and 12 of DSS-induced colitis. (*A*) Bacterial families. (*B*-*E*) Bacterial genera of the following families: (*B*) *Ruminococcaceae*. (*C*) *Lachnospiraceae*. (*D*) *Prevotellaceae*. (*E*) *Porphyromonadaceae*. The data are means ± SEM. The two-sided Wilcoxon rank-sum test was performed for analysis. **P*<0.05, ***P*<0.01.

Figure S10: Gut barrier impairment in germ-free mice colonized with faecal microbiota from *REG3A*-transgenic (ExGF-TG; n=8) and WT (ExGF-WT; n=8) mice during DSS-induced colitis. Histological assessment of gut epithelium (n=8 for each group). The data are means ± SEM. *P*=ns (Wilcoxon rank-sum test).

Figure S11: Representative colon images from WT mice exposed to TNBS and administered 100µg of a recombinant REG3A protein (rcREG3A) or an equivalent volume of buffer intrarectally. Staining: hematoxylin and eosin. Top row: full views of the same colon sections as in Figure 6*B*. Scale bar, 1mm.

Supplemental Document 1 - Materials and Methods

Animal studies

Animal studies were performed in compliance with the institutional and European Union guidelines for laboratory animal care and approved by the Ethics Committee of CE2A-03 CNRS-Orléans (Accreditation N°01417.01). The number of *Mus musculus* mice used was in compliance with institutional ethical rules and consistent with common practice in the fields of microbiota analysis and experimental colitis. Conventional mice were produced and housed in the CNRS SEAT and Institut André Lwoff animal care facilities (Université Paris-Sud, Villejuif). Germ-free mice were housed at the Anaxem platform of the Micalis Institute (INRA, Jouy-En-Josas). All the conventionally bred mouse groups were homogeneous in terms of age (10-12 weeks), weight (25g), sex (50% male and 50% female) and environmental factors. All the *REG3A*-transgenic mice had circulating hREG3A levels within the 200-600ng/mL range. None was excluded from the study. Wild-type and *REG3A*-transgenic mice had the same C57BL/6N genetic background. They were not littermates. WT female mice were crossed with *REG3A* homozygous males to generate heterozygous pups harbouring the maternal microbiota at birth. For the cohousing experiments, 3-week-old weaned *REG3A*-transgenic mice were cohoused randomly with age-matched WT mice at a 1:1 ratio for 8 weeks. Some of these mice were exposed to DSS, while others were used for tissue analysis at the end of the cohousing period. For the faeces transfer experiments, male germ-free C57BL/6 mice were housed in sterile isolators. Their germ-free status was checked weekly using microbiological assays on faeces and drinking water. At the age of 10 weeks, the germ-free mice underwent two gastric gavages at 48h intervals, using 0.5 mL of inoculum prepared from conventional mice faecal microbiota diluted 1/100. Inocula consisted of pooled faeces from 8 transgenic or 8 WT mice. To induce colitis, mice were fed with a 3% 40kDa

dextran sodium sulphate (DSS) solution (TdB Consultancy AB) added to their drinking water for 5 days (solution changed every day). The animals were then fed with tap water for 7 additional days. Weight loss, stool consistency and bleeding were evaluated daily. Scores are defined as follows: stool consistency: 0 (normal), 1 (soft), 2 (very soft), 3 (diarrhea); stool bleeding: 0 (normal), 1 (red), 2 (dark red), 3 (gross bleeding). For colitis induction by 2,4,6-trinitrobenzene sulfonic acid (TNBS; Sigma-Aldrich), overnight-fasted mice were anesthetized for 90 min and received a single intrarectal administration of TNBS (40µl, 150 mg/kg) dissolved in a 1:1 mixture of 0.9% NaCl with 100% ethanol. Control mice received a 1:1 mixture of 0.9% NaCl with 100% ethanol. The WT mice that were administered the recombinant hREG3A protein received an intrarectal injection of 100µg of rcREG3A on the day before and on the day of TNBS administration. Macroscopic examination, histological analysis and qPCR were performed 2 days after TNBS administration. The different mouse groups (WT or transgenic, single-housed or cohoused, conventionally fed or germ-free) were used exhaustively.

Composition of the microbiota

DNA pyrosequencing of the V3-V4 hypervariable region of 16S rRNA gene was performed using the Illumina Miseq instrument. The sequences thus generated were pre-processed using the mothur pipeline and then clustered into OTUs based on 97% of similarity. Using the RDP Classifier, we assigned OTUs to taxa (genus-level) with a confidence threshold of 80%. RDP release 11 was used as the reference database. Principal Component Analyses (PCA) were performed based on bacterial family and genera compositions using the R packages ade4 and FactoMiner. Families representing more than 0.5% of the total bacterial population were taken into account. The robustness of each clustering result was assessed using a Monte-Carlo rank test (B= 999 repetitions, $p < 0.05$). Differences between groups were analysed using a

non-parametric Wilcoxon rank sum test. All the relevant data can be found in the text, except for the DNA sequence reads, which are available from the Sequence Read Archive (accession numbers pending) or by contacting the corresponding author.

Bacterial strains, culture conditions and flow cytometry

Gram-positive *Enterococcus faecalis* ATCC-19433 were grown at 37°C under shaking in BHI (BD Bacto™ Brain Heart Infusion) broth overnight and then in LB (Luria-Bertani; Becton Dickinson). To induce peroxide stress on *E. faecalis*, 5.10^6 bacteria per mL were incubated at 37°C with 200mM Paraquat (1,1′-dimethyl-4,4′-bipyridinium dichloride; Sigma Aldrich) and 10µM of a recombinant hREG3A (rcREG3A) protein or equivalent volume of buffer. The reagents were added to the culture during the log phase. Colony-forming units (CFUs) were counted after plating serial dilutions on LB agar plates incubated at 37°C overnight. All cultures were performed in quadruplicate during three independent experiments. Intracellular ROS levels and cell viability were determined by flow cytometry with 2′,7′-dichlorofluorescein diacetate (H_2-DCFDA; Life Technologies) and propidium iodide (Sigma Aldrich) in *E. faecalis* cultures incubated with paraquat alone or paraquat supplemented with 10µM rcREG3A for 8h. H_2-DCFDA was dissolved in dimethyl sulphoxide (DMSO; Sigma) to 10mM and added at a final concentration of 10µM. After incubating *E. faecalis* cultures for 30 min. in the dark at 37°C, the cells were pelleted, washed twice with PBS, suspended in 1 mL PBS supplemented with 1µg/mL propidium iodide and processed in a BD Accurri C6 flow cytometer (Becton Dickinson). For the measurements of bacterial ROS levels in faecal microbiota, fresh faeces were suspended in cold PBS and centrifuged twice at 2000 rpm for 5 min at 4°C. The supernatant was incubated with PBS containing 25 µM H_2-DCFDA for 15 min and then centrifuged at 5000 rpm for 5 min. The resulting pellet was suspended in cold PBS and processed in the flow cytometer. Analysis of the flow data was performed using

Flow Jo software. *Faecalibacterium prausnitzii* A2-165 (DSM17677) and *Roseburia intestinalis* L1-82 (DSM14610T) were grown under strict anaerobic conditions at 37°C for 24h in LYHBHI medium (BHI broth supplemented with 0.5% yeast extract and 5mg/L hemin) supplemented with 1mg/mL maltose, 1mg/mL cellobiose and 0.5mg/mL cysteine-HCl.. Anaerobic growth of *F. prausnitzii* and *R. intestinalis* was performed in the presence of 5µM of rcREG3A for 7h or 24h, respectively, and followed by a 5-min exposure to ambient air. Bacterial growth was assessed by CFU counting on agar plates. CFU numbers were normalized to the average CFU number measured in control cultures (buffer). Protein extracts from *F. prausnitzii* grown for 2h or 24h with rcREG3A or buffer were subjected to SDS-PAGE. Each experiment was performed in quadruplicate during three independent experiments. Wet mounts were observed using a Deltavision optical microscope with a 63x objective lens.

Recombinant REG3A proteins

Two batches of recombinant proteins were used; one (ALF5755) supplied by the Alfact Innovation Company and the other made in our laboratory. We subcloned the coding sequence corresponding to the secreted form of hREG3A within pET28-N-HIS-SUMO (Novagen). The resulting construct was verified by sequencing and then transformed into an engineered *Escherichia coli* BL21 (DE3) strain co-expressing the sulfhydryl oxidase Erv1p and the disulphide isomerase DsbC. These modifications enabled the efficient production of natively folded hREG3A in the cytoplasm. The hREG3A proteins were produced in a 7L Infors-Labfors fermenter at 20°C and pH 6.8 ± 0.1 for 16h. These cells were then pelleted and lysed using a one-shot desintegrator (CellD) at 1.5 kbar. The proteins were purified from the supernatant using Ni-NTA resin (Macherey Nagel), cleaved with a home-made SUMO

protease. The His-tag and Sumo protease were removed from the protein suspension by a Ni-NTA resin. The resulting supernatant was dialysed against 50 mM phosphate buffer pH7.4.

ELISA assays

The serum concentrations of Reg3g, hREG3A, lipopolysaccharides (LPS) and soluble CD14 were measured using the E94676Mu (Uscn Life Science Inc.), PancrePAP (Dynabio), LAL chromogenic endpoint (Hycult biotech) and One Step ELISA (BioMetec) kits, respectively, according to the manufacturer's instructions. The myeloperoxidase concentration in colon tissues homogenates was determined using the mouse MPO ELISA kit (Hycult biotech).

Histological analysis

For each mouse studied, two samples from the distal and proximal colon were fixed in 4% paraformaldehyde acid and then embedded in paraffin. 4-µm-thick sections were deparaffinized in xylene for 5 min. and rehydrated for 5 min. in 100%, 90% and 70% ethanol successively. They were then stained with hematoxylin/eosin/alcian blue, randomly sorted and scored in a blind manner by an expert in pathology. The score used for DSS-induced colitis was as follows. Grade 0: normal mucosa; Grade 1: infiltration of inflammatory cells; Grade 2: crypt abscesses and erosion, and Grade 3: destruction of epithelial cells (ulceration and loss of Goblet cells). The number of sections analysed per colon sample ranged from 2 to 6. The Ameho score used for TNBS-induced colitis reads: Score 0: no lesion; Score 1: mild mucosal or submucosal inflammatory infiltrate with edema. Punctuate mucosal erosions. Muscularis mucosae intact; Score 2: score 1 changes involving 50% of the specimen; Score 3: prominent inflammatory infiltrate with deeper areas of ulceration extending through the muscularis mucosae into the submucosa.; Score 4: score 3 changes involving 50% of the

specimen; Score 5: extensive ulceration with coagulative necrosis extending deeply into the muscularis mucosae; Score 6: score 5 changes involving 50% of the specimen.

Immunohistochemistry

Formalin-fixed, paraffin-embedded colon sections (4 µm) were de-waxed in xylene and rehydrated through graded alcohols. Tissue sections were pressure cooked in 10mM citrate buffer pH6 for 5 min., incubated with 3% H_2O_2 for 20 min. to block endogenous peroxidase and then incubated with a laboratory-made purified rabbit polyclonal anti-hREG3A antibody[1]. Secondary anti-rabbit IgG-HRP was used according to the manufacturer's instructions (DAKO). The sections were counter-stained with alcian blue (Sigma) before mounting the coverslips.

Lipid peroxidation

Malondialdehyde (MDA) was dosed using the thiobarbituric acid method as previously described[1]. A standard curve was prepared using Malondialdehyde Tetrabutylammonium Salt (Sigma Aldrich, Lyon, France). The results were normalized in relation to the total protein content.

In situ hybridisation and Immunofluorescence

Unwashed segments of colon and mesenteric lymph nodes were fixed in methanol-Carnoy mixture, followed by embedding in paraffin. Paraffin sections (3 to 5µm) were de-waxed and washed in 100% ethanol. In situ hybridization (FISH) was performed as previously described[2]. The oligonucleotide probes used are EUB338 and univ1390 for universal 16S RNA (See the probeBase online resource). Bacterial translocation levels in mesenteric lymph nodes were determined on FISH images in at least 1-2 lymph nodes per mouse and 3 sections

per node. Anti-Mucin2 antibody (H300, sc-15334, Santa Cruz) was used at a dilution of 1:100 in 4% goat serum. The Muc2 signal was detected using a goat anti-rabbit IgG-Alexa 598 (A11036, Molecular probes). The tissues were counter-stained with DAPI and fluorescent images were acquired using a Deltavision real-time microscope piloted by SoftWorx software (Applied Precision, GE Healthcare), with a 40x/1.4NA objective (Olympus) and a CDD CoolSNAP HQ2 camera (Photometrics).

Transcriptomics, quantitative PCR

RNAs were purified from colon tissues using the mirVana miRNA isolation kit (Ambion). RNA quality was evaluated with the Agilent 2100 bioanalyzer. Samples with an RNA integrity number (RIN) higher than 7 were processed for transcriptomic analysis. Biotinylated single strand cDNA targets were prepared from 200 ng total RNA using the Ambion® WT Expression Kit and the Affymetrix GeneChip® WT Terminal Labeling Kit, according to the manufacturer's instructions. 1.9 µg of cDNAs were hybridized for 16h at 45°C on GeneChip® Mouse Gene 1.0 ST arrays (Affymetrix) interrogating 28.853 genes represented by approximately 27 probes spread along the full length of the gene. The chips were washed and stained in the GeneChip® Fluidics Station 450, and scanned with the GeneChip® Scanner 3000 7G at a resolution of 0.7 µm. CEL files were further processed with Affymetrix Expression Console software version 1.1 to calculate the probe set signal intensities using Robust Multi-array Average (RMA) algorithms with default settings. Transcriptomic data have been deposited in Gene Expression Omnibus (NCBI) under the accession number GSE64932. For quantitative PCR, the sequences of the specific primers used were as follows. Tnf-F: GGGAGTAGACAAGGTACAAC; Tnf-R: TCTCATCAGTTCTATGGCCC. Il1-F: CAACCAACAAGTGATATTCTCCATG; Il1-R: GATCCACACTCTCCAGCTGCA. Hprt-F: AGGACCTCTCGAAGTGT; Hprt-R: TCAATCCCTGAAGTACTCAT.

Gene set enrichment analysis

GSEA was performed to explore the gene sets differentially expressed between wild-type and *REG3A*-transgenic mice. GSEA version 2.0 software was downloaded from the Broad Institute website, working with Version 4.0 of MsigDB. The most significant gene sets are displayed with their corresponding normalized enrichment scores (NES) and nominal p-values. Medline/PubMed data mining for LPS-endotoxin functionality was performed using LPS and endotoxin as the keywords. 356 genes with a raw *P*-value <0.05 were retrieved from 4267 articles. 85 genes were still related to LPS-induced cellular responses after correction of the multi-testing error by the false discovery rate. Unsupervised hierarchical clustering (Euclidean distance and complete linkage) was performed using the expression profiles of the 85-gene set.

Immunoblotting

The quantification of hREG3A protein along the GI tract of *REG3A*-transgenic mice was performed using the anti-hREG3Aimmunoblotting of 50 µg total protein. Immunodetection of the recombinant hREG3A protein (rcREG3A) in bacterial cultures was performed by spinning down 200 µL of a bacterial culture previously incubated with rcREG3A or buffer for 2h or 24h. The pellet was washed three times with PBS supplemented with a protease inhibitor cocktail (eComplete, Roche), re-suspended in 30 µL Laemmli buffer and stored at -20°C. After denaturation for 5 min. at 95°C, the sample extracts were separated on 15% polyacrylamide gel by SDS-PAGE, and then transferred onto a nitrocellulose membrane for immunoblotting using our anti-hREG3A antibody. Total protein lysates were extracted from mouse colon tissues with RIPA buffer (50mM Tris-Cl pH7.4, 150 mM NaCl, 1% NP40, 0.25% sodium deoxycholate, protease inhibitors). To detect O-glycoproteins containing Core

3, 500ng protein were resolved on 4-15% precast polyacrylamide gel (Bio-rad), electro-transferred onto a nitrocellulose membrane and hybridized with wheat germ agglutinin (WGA) conjugated with horseradish peroxidase (HRP) (Sigma Aldrich).

Dot blot

Monosaccharides (glucose, mannose) and polysaccharides (LPS, peptidoglycan, mannan, DSS) (Sigma Aldrich) at two doses (30ng, 150ng) were spotted onto nitrocellulose membranes and cross-linked to the membrane using UV irradiation. The membranes were washed twice with PBS, and hybridized with 1µg/mL of recombinant hREG3A protein (rcREG3A) at 37°C for 2h. Non-hybridized hREG3A proteins were washed away with TBST (50mM Tris-Cl pH7.4, 150 mM NaCl, 0.1% Tween), The membranes were incubated with our anti-hREG3A antibody for 30 min. at RT and then with HRP conjugated goat anti-rabbit antibody to reveal the hREG3A proteins attached to saccharides.

[^{18}F]FDG PET scan

[^{18}F]FDG was purchased from Cyclopharma S.A. (Clermont-Limagne, France). The mice to be imaged were anaesthetized with oxygen-isoflurane (2% isoflurane, 0.4 L/min. oxygen) and kept at a physiological body temperature on a heating pad. Three male WT and *REG3A*-transgenic mice were injected intravenously with 10 MBq [^{18}F]FDG in 100 µL PBS on different days of induced colitis. The images were acquired dynamically over 15 min. as from 1h after the radioisotope injection, using a microPET Focus (Siemens). The uptake of radioactivity was quantified in regions of interest (ROI) drawn in the abdominal areas of the reconstructed PET images. For each ROI, the mean uptake was calculated as the percent-injected dose per gram tissue (%ID/g) assuming a tissue density of 1g/cm^3.

Statistics

Results are presented as means ± SEM or box plots. Differences between sample groups were tested using non-parametric Wilcoxon rank sum (two-sided) for all the experiments reported, with the following exceptions: Two-way ANOVA tests were used for the in-vivo quantifications of [^{18}F]FDG and H_2-DCFDA over time; the robustness of Principal Component Analysis clustering was assessed with a Monte-Carlo rank test; the Kaplan-Meier survival analysis with a log-rank test was applied to compare the time course of survival between the groups. *P*-values <0.05 were considered to be statistically significant.

Supplemental References

1. Moniaux N, Song H, Darnaud M, et al. Human hepatocarcinoma-intestine-pancreas/pancreatitis-associated protein cures fas-induced acute liver failure in mice by attenuating free-radical damage in injured livers. Hepatology 2011;53:618–627.

2. Canny G, Swidsinski A, McCormick BA. Interactions of intestinal epithelial cells with bacteria and immune cells: methods to characterize microflora and functional consequences. Methods Mol Biol 2006;341:17–35.